

MobileManiBench: Simplifying Model Verification for Mobile Manipulation

Wenbo Wang² Fangyun Wei^{1*} Qixiu Li³ Xi Chen¹
 Yaobo Liang¹ Chang Xu² Jiaolong Yang¹ Baining Guo¹

¹Microsoft Research Asia ²University of Sydney ³Tsinghua University

{fawe, xichen6, yalia, jiaoyan, bainguo}@microsoft.com

wwan0412@uni.sydney.edu.au liqx23@mails.tsinghua.edu.cn c.xu@sydney.edu.au

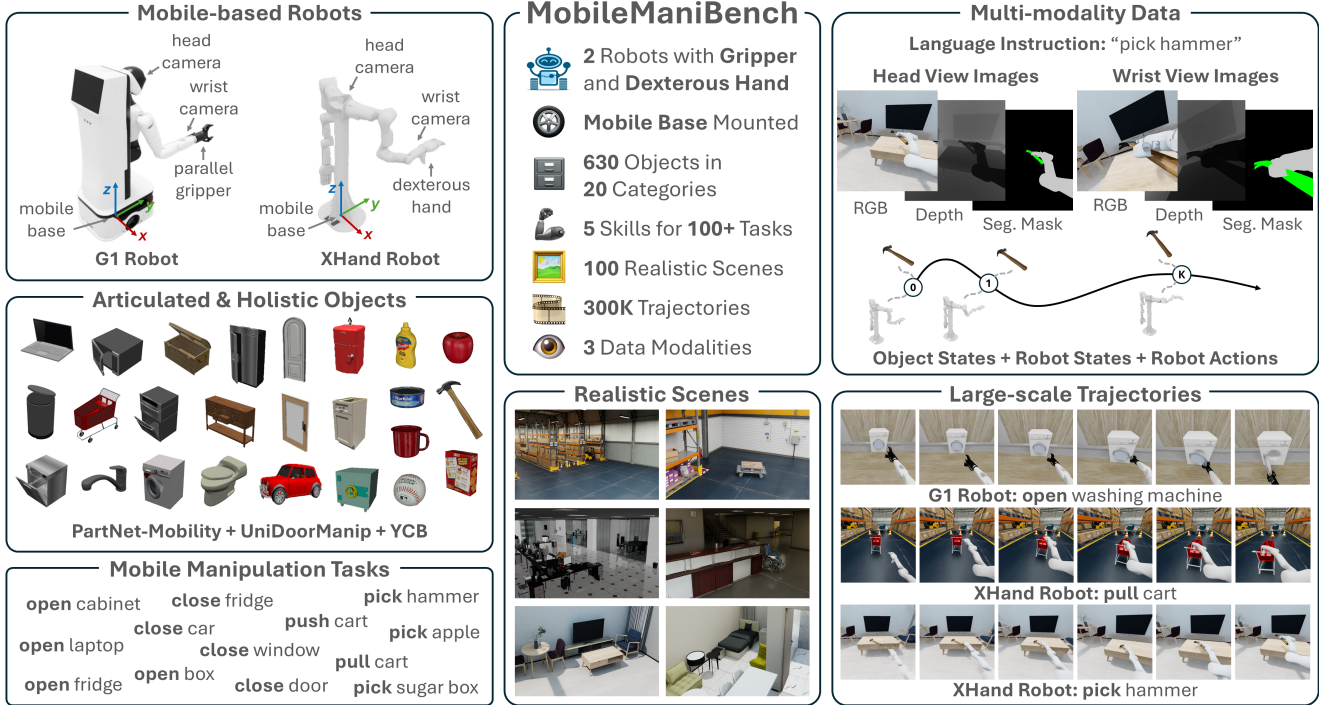


Figure 1. Overview of **MobileManiBench**. It features 2 mobile-based robots: the G1 robot with a parallel gripper and the XHand robot with a dexterous hand. The benchmark includes 630 articulated and holistic objects across 20 categories and supports 5 mobile manipulation skills—open, close, pull, push, and pick—enabling over 100 tasks. To efficiently scale data generation while ensuring task success, we train a universal **MobileManiRL** policy for each robot–object–skill triplet and generate **MobileManiDataset** across 100 realistic scenes with 300K trajectories and 3 data modalities—language instructions, multi-view RGB–depth–segmentation images, synchronized object/robot states and actions. MobileManiBench offers a flexible testbed to accelerate model innovation and data-efficiency research for VLA models.

Abstract

Vision-language-action models have advanced robotic manipulation but remain constrained by reliance on the large, teleoperation-collected datasets dominated by the static, tabletop scenes. We propose a simulation-first framework to verify VLA architectures before real-world deployment and introduce MobileManiBench, a large-scale benchmark for mobile-based robotic manipulation. Built on NVIDIA Isaac Sim and powered by reinforcement learning, our pipeline autonomously generates diverse manipulation trajectories with rich annotations (language instructions, multi-view RGB–depth–segmentation images, synchronized object/robot states and actions). MobileManiBench fea-

tures 2 mobile platforms (parallel-gripper and dexterous-hand robots), 2 synchronized cameras (head and right wrist), 630 objects in 20 categories, 5 skills (open, close, pull, push, pick) with over 100 tasks performed in 100 realistic scenes, yielding 300K trajectories. This design enables controlled, scalable studies of robot embodiments, sensing modalities, and policy architectures, accelerating research on data efficiency and generalization. We benchmark representative VLA models and report insights into perception, reasoning, and control in complex simulated environments, with all code, datasets, and models publicly released at https://dexhand.github.io/MobileManiBench_Website/.

1. Introduction

Recent advances in Vision-Language-Action models [4–6, 8, 17, 22–25, 30, 34, 35, 38, 42, 44, 48, 49, 51, 54, 57, 59] have substantially advanced robotic manipulation, demonstrating strong generalization to novel objects and diverse visual domains. However, the success of current VLA models heavily dependents on large-scale datasets, among which, the *openX-Embodiment* dataset [34] has become the de facto training resource. Yet, most of its data are collected via teleoperation from static, third-person or head-mounted viewpoints, restricted to indoor tabletop environments populated with a limited set of household objects. These constraints introduce several challenges:

- Any modification to the hardware configuration—such as incorporating new sensors (e.g., depth or wrist-mounted cameras), extending to mobile-based manipulation, or replacing grippers with dexterous hands—necessitates recollecting data from scratch. If these additions fail to provide substantial performance gains, the effort becomes wasteful due to the high cost and inefficiency of teleoperation-based data collection.
- Although teleoperation pipelines are effective for simple gripper-based robots, they become cumbersome when scaled to dexterous or mobile platforms, thereby impeding rapid model development and iteration.

To support scalable *verification* of VLA architectures, we propose conducting data generation and evaluation in simulation environments prior to collecting real-world robotic data. The key idea is to offer an efficient way to scale up objects, tasks, and scenes, while flexibly supporting diverse robot configurations—such as dexterous hands, mobile bases, arbitrary camera placements—and easily acquiring multi-modal sensory inputs (e.g., RGB, depth, robot proprioception). In this work, we leverage *NVIDIA Isaac Sim* [33] as the simulation platform and employ reinforcement learning [37] to train agents that can automatically generate manipulation trajectories along with corresponding annotations (e.g., text instructions, camera images, and robot states). Building upon this automated pipeline, we introduce **MobileManiBench**—a large-scale benchmark for mobile manipulation and embodied skill learning.

As shown in Figure 1, MobileManiBench is designed with several distinguishing features:

- *Multi-Robot Embodiment*: Two robot platforms are provided—one equipped with a parallel gripper and another with a dexterous anthropomorphic hand.
- *Mobile-Base Platform*: Both robots are mounted with a mobile base, allowing for spatially extended tasks that require coordinated navigation and manipulation.
- *Rich Visual Sensing*: Two cameras are mounted on the head and right wrist, each capturing synchronized RGB, depth, and segmentation images to facilitate multi-view and multi-sensory perception.

- *Multi-Modality Trajectories*: Each recorded trajectory includes textual instructions, multi-view visual images, together with object states, robot states and actions, forming comprehensive supervision signals for VLA training.
- *Diverse and Scalable Content*: The dataset contains 630 unique objects spanning 20 categories, 100 realistic and semi-structured scenes, 5 mobile manipulation skills across 100 tasks, and generates over 300K trajectories.

The above design enables controlled experimentation with different robot configurations, sensory modalities, and model architectures, without requiring expensive real-world data collection. Researchers can efficiently evaluate whether new input modalities (e.g., wrist images or depth images) contribute to better manipulation performance or whether specific architectural designs improve multi-sensory fusion and reasoning. MobileManiBench thus provides a flexible testbed for accelerating both model innovation and data-efficiency exploration in embodied AI.

Leveraging MobileManiBench, we systematically compare several existing VLA models [5, 17, 21, 23] with our proposed MobileManiVLA, analyze their strengths and weaknesses across various tasks, and provide a series of empirical takeaways that offer new insights into how large-scale multi-modal architectures perceive and act in complex robotic manipulation environments. We hope that this benchmark will foster reproducible research, enable rapid architectural iteration, and pave the way toward scalable, general-purpose VLA models.

2. Related Works

Robotic Manipulation Benchmarks. Robotic manipulation [1, 2, 9, 10, 14, 15, 18, 20, 27, 32, 46, 53, 55] remains a central challenge in embodied AI. Existing datasets and benchmarks can be broadly categorized into two groups, as summarized in Table 1. The first group comprises real-world datasets and evaluation protocols, such as DROID [20], AgiBotWorld-Beta [1] and Open X-Embodiment [34], which collect large-scale manipulation trajectories through extensive teleoperation or by aggregating data from multiple robot platforms. Despite their impressive scale, these works primarily focus on fixed-base or gripper-equipped robots performing mostly tabletop tasks. Recent efforts like DexGraspVLA [57], Humanoid Everyday [55], and Mobile ALOHA [14] extend to dexterous hands and mobile manipulation, yet still rely on real-world human teleoperation, which limits their diversity and scalability. Overall, real-world data collection and model evaluation remain costly and risky, as they require complex scene setups and pose a high risk of hardware damage. Moreover, although existing real-world benchmarks cover a variety of manipulation skills, their evaluations are often limited to a narrow subset of tasks, leading to imbalanced training and testing coverage across object categories and skills.

Benchmarks / Datasets	Object Number	Object Category [†]	Skill Number ^{††}	Scene Number	Trajectory Number	Mobile Based	Parallel Gripper	Dexterous Hand	Articulated Object	Universal Model ^{†††}
DROID [20]	*	*	86	564	76K		✓		✓	
Open X-Embodiment [34]	5228	*	527	311	1400K		✓		✓	✓
AgiBotWorld-Beta [1]	3000	*	87	106	1000K		✓	✓	✓	✓
DexGraspVLA [57]	36	1 [†]	1	-	2K		✓	✓		✓
Humanoid Everyday [55]	*	*	221	*	10.3K	✓		✓	✓	✓
Mobile-ALOHA [14]	6	6	6	6	300	✓	✓		✓	
DexArt [2]	82	4	2	1	/			✓	✓	
RLBench [18]	*	*	30	1	/		✓		✓	
Robosuite [58]	10	*	10	1	/		✓		✓	
SIMPLER [26]	17	2	4	-	/		✓		✓	✓
RoboTwin 2.0 [10]	731	10	11	-	100K		✓		✓	✓
VLABench [53]	2164	10	11	-	5K		✓		✓	✓
LIBERO [28]	75	*	*	20	6.5K		✓		✓	✓
CALVIN [31]	30	5	10	4	20K		✓		✓	✓
Maniskill2 [15]	2144	*	12	*	30K	✓	✓		✓	
RoboCasa [32]	2509	8	8	120	100K	✓	✓		✓	
UniDoorManip [27]	328	6	1	1	/	✓	✓		✓	✓
OWMM-Agent [9]	157	1 [†]	2	143	21K	✓	✓			✓
GRUtopia [45]	2956	1 [†]	2	100	900	✓	✓	✓		
MobileManiBench (Ours)	630	20	5	100	300K	✓	✓	✓	✓	✓

Table 1. Comparison of existing robotic manipulation benchmarks and datasets. The top rows correspond to real-world datasets, while the bottom rows refer to simulation-based works. *Object Category[†]* treats holistic objects (e.g., apples, bottles, toys) as single categories. *Skill Number^{††}* denotes the set of manipulation verbs included. *Universal Model^{†††}* indicates whether a universal policy has been trained within the benchmark. A “-” in *Scene Number* indicates that the work uses a single tabletop layout with varying textures. A “/” in *Trajectory Number* indicates that users must generate the trajectories themselves. An asterisk “*” denotes statistics not reported in the original paper. AgiBotWorld-Beta collects real-world G1-robot data through teleoperation, with only a small number of mobile-manipulation examples.

The second group [2, 9, 10, 15, 18, 26–28, 31, 32, 45, 47, 53, 58] alleviates the above limitation by leveraging high-fidelity simulation environments to simulate diverse manipulation tasks, collect large-scale trajectories, and perform extensive model evaluations. These methods typically collect data either through simulation-based teleoperation or by designing task-specific agents using rule-based methods or reinforcement learning (RL) policies. While simulation greatly reduces the cost and risk, there remains a lack of large-scale, multi-modality trajectory datasets that support training universal models capable of generalizing across diverse object categories, manipulation skills, and realistic scenes. MobileManiBench follows this simulation-based paradigm, leveraging the high-fidelity NVIDIA *Isaac Sim* [33] and a diverse set of digital assets to train universal RL policies across various robot–object–skill combinations. It supports large-scale trajectory generation in diverse realistic digital scenes, facilitating scalable model training and evaluation for mobile-based robotic manipulation with both parallel grippers and dexterous hands.

Vision-language-action Models. VLA models [4–6, 8, 17, 22–25, 30, 34, 35, 38, 42, 44, 48, 49, 51, 54, 56, 57, 59] have emerged as a promising framework for learning universal robotic policies that generalize across diverse objects, tasks, and scenes. Recent works [4, 5, 17, 23, 49] advance this direction by integrating vision–language (VL) backbones [3, 11, 13, 19, 29, 40] with diffusion-based or flow-matching-based action modules. By combining the

pretrained VL priors, multi-modality representations, and continuous action modeling, these approaches substantially lead the robotic manipulation performance.

However, existing VLA models are mostly trained and evaluated on fixed-base, gripper-equipped robots performing tabletop manipulation tasks, with limited examples of dexterous hands or mobile-based manipulation [6, 8, 22, 23, 25, 30, 34, 35, 38, 42, 44, 48, 49, 51, 54, 57, 59]. MobileManiBench extends this research by providing large-scale synthetic trajectories for mobile-based robots equipped with either parallel grippers or dexterous hands, covering diverse objects, tasks, and scenes. It systematically studies the effect of different model structures and input modalities on mobile manipulation performance, filling a critical gap in current VLA research.

3. Problem Formulation

Mobile-based Robot. MobileManiBench employs two mobile-based robots: the G1 robot from AGIBOT [?] and the XHand robot from RobotEra [36], as shown in Figure 1. Although both robots are equipped with dual arms, we fix the left arm and activate only the right arm for manipulation. Each robot has a 7-DOF right arm and a 2-DOF mobile base (one rotational DOF around the z-axis and one translational DOF along the y-axis). The G1 robot uses a parallel gripper with 1 DOF as its end effector, whereas the XHand robot is equipped with a dexterous 12-DOF hand. Both robots are controlled using (6+D) dimensional actions, where the first

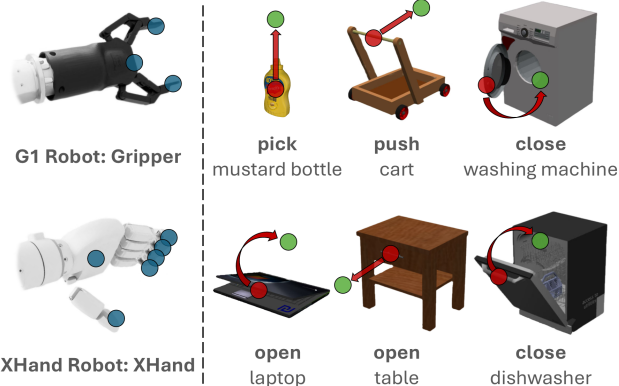


Figure 2. Definitions of the robot gripper/hand points (blue), object grasp point (red), and goal point (green) across diverse tasks.

6 dimensions represent the wrist pose displacement relative to the previous frame, from which inverse kinematics computes the target joint angles of mobile base and right arm. The remaining D dimensions correspond to the target joint angles of end effector. This formulation yields 7-d actions for the G1 robot and 18-d actions for the XHand robot.

Mobile-based Manipulation Objects, Skills, and Tasks. MobileManiBench encompasses both the articulated and holistic objects sourced from the PartNet-Mobility [50], UniDoorManip [27], and YCB [7] datasets, totaling 630 objects across 20 categories (holistic objects such as apples, bottles, and toys are grouped into a single “holistic” category). We define five mobile manipulation skills: *open* and *close* for objects including boxes, toilets, laptops, trash-cans, dishwashers, ovens, microwaves, refrigerators, washing machines, cars, safes, fridges, cabinets, windows, lever doors, round doors, faucets, and tables; *pull* and *push* for carts; and *pick* for holistic (YCB) objects. This formulation yields over 100 distinct tasks for large-scale data collection and model training, including tasks such as opening a laptop, closing a cabinet, pushing a cart, pulling a cart, picking an apple, and picking a mustard bottle.

4. Method

Overview. The construction of MobileManiBench consists of two stages. First, in the *MobileManiRL Training* stage (Section 4.1), we train a state-based reinforcement learning (RL) policy for each robot–object–skill combination, covering robots equipped with either a parallel gripper or a dexterous hand. Second, in the *MobileManiDataset Generation* stage (Section 4.2), each trained RL policy is deployed in diverse digital scenes to collect successful manipulation trajectories. Each trajectory includes a natural language instruction paired with synchronized multi-modal data: multi-view camera images, object states, robot states, and actions.

Building on *MobileManiDataset*, we further introduce *MobileManiVLA* (Section 4.3), where all trajectories across robot–object–skill–scene combinations are aggregated to

Input Type	G1 Robot	XHand Robot
Time	30	30
Object State	9	9
Robot Proprioception	78	135
Robot-Object Distance	22	31
Previous Action	7	18

Table 2. Dimensions of the input types used in MobileManiRL for the G1 and XHand robots. Detailed definitions of each input element are provided in the Appendix.

train a universal vision-language-action model for each robot, enabling strong generalization to unseen objects and unseen scenes.

4.1. MobileManiRL Training

Given that our benchmark involves 2 mobile-based robots, 630 objects across 20 categories, 5 manipulation skills, and over 100 tasks, teleoperating or manually designing policies for each configuration would be prohibitively time-consuming. To address this, we propose a universal state-based reinforcement learning (RL) policy, termed *MobileManiRL*, which parameterizes each robot–object–skill combination using keypoint-based displacements of the robot gripper/hand points, the object grasp point, and the goal point [16, 52], as illustrated in Figure 2. A universal reward function R encourages the robot’s gripper/hand points to reach the object grasp point and transport it to the goal point. This formulation enables a single RL policy to generalize across diverse manipulation scenarios while maintaining task-specific success.

Inputs. Table 2 summarizes the five input types used in MobileManiRL. Specifically, *Time* encodes the timestep embedding; *Object State* represents the states of the object grasp point and goal point; *Robot Proprioception* captures the robot’s body and joint states; *Robot-Object Distance* measures the distances between the robot gripper/hand points and the object grasp point; and *Previous Action* records the previous (6+D)-dimensional action.

Network Architecture. Each MobileManiRL policy network is a 4-layer MLP with hidden dimensions of $\{1024, 1024, 512, 512\}$, followed by an action prediction head implemented as a single fully connected layer. This head outputs a (6+D) dimensional vector (7-d for the G1 robot and 18-d for the XHand robot) representing the action at the current time step. The value network adopts the same architecture as the policy network but outputs a single scalar.

Reward Function. The reward function R is designed as:

$$R = R_d + (1 - f_g)R_a + f_g(R_g + R_m + R_s), \quad (1)$$

where the global distance reward R_d penalizes the distances between the gripper/hand points and the object grasp point, as well as between the object grasp point and the goal point, encouraging the robot to grasp the object and move it to-

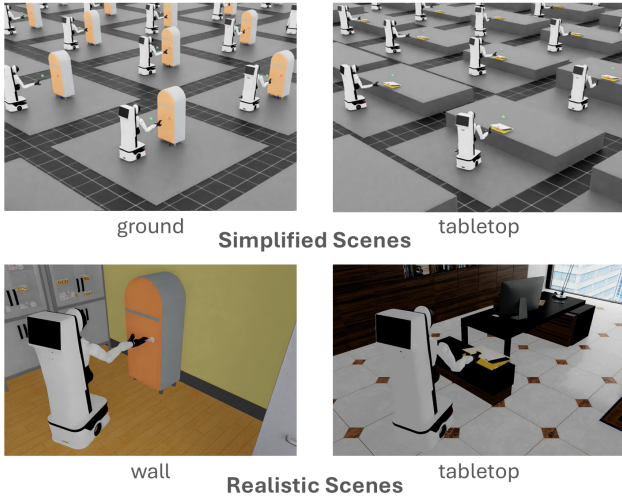


Figure 3. Illustrations of simplified scenes for MobileManiRL training and realistic scenes for MobileManiDataset generation and MobileManiVLA evaluation.

ward the goal. The grasp flag f_g is set to 1 when the distance between the gripper/hand points and the object grasp point falls below a predefined threshold. The approach action reward R_a guides the gripper/hand toward the object grasp point via a reference approach action until a grasp is achieved. Once grasped (i.e., $f_g = 1$), the grasp reward R_g provides a bonus; the move action reward R_m encourages the gripper/hand to move to the goal point via a reference move action; finally the success reward R_s provides an extra bonus when the object reaches the goal. Formal definitions of all reward elements are provided in the Appendix. A manipulation is considered successful if the object grasp point reaches the goal point within $T = 300$ steps.

Simplified Scene Training. We place the 20 categories of objects into 2 simplified scene settings in Isaac Sim and train one MobileManiRL policy for each robot-object-skill combination, as shown in Figure 3. The *ground* scene includes toilet, trashcan, refrigerator, washing machine, car, fridge, cabinet, window, lever door, round door, table, and cart; while the *tabletop* scene includes box, laptop, dishwasher, oven, microwave, safe, faucet, and holistic (YCB) objects. Each object is initialized either on the ground or on the tabletop with random heights, facing the negative y axis, and with its grasp point’s x-y coordinates set to zero. The robot mobile base is initialized facing the object grasp point with random positional offsets (1.0m to 1.5m along the x and y axes) and rotational offsets (-15° to 15° around the z axis) to enhance policy robustness. Under this setup, we train MobileManiRL on each of the 1,182 robot-object-skill combinations for both G1 robot and XHand robot, achieving mean success rates of **89.6%** and **92.9%**, respectively.

4.2. MobileManiDataset Generation

Realistic Scene Rendering. Each trained MobileManiRL policy is now able to perform its assigned robot-object-skill

across diverse robot initial poses. We then place the 20 categories of objects into 5 realistic scene settings for trajectory rendering: space (cart), wall (toilet, trashcan, refrigerator, washing machine, fridge, cabinet, table), door (window, lever door, round door), outdoor (car), and tabletop (box, laptop, dishwasher, oven, microwave, safe, faucet, holistic objects). For each scene setting, we manually annotate 20 scene placements using digital assets from the Isaac Sim [33] and Genie Sim [43], yielding a total of 80 seen scene placements for VLA training and 20 unseen reserved for testing. These scenes cover a variety of everyday environments, including kitchen, bedroom, hospital, office, warehouse, and parking lot, as shown in the Appendix.

Dataset Analysis. For each of the G1 robot and the XHand robot, MobileManiDataset comprises 630 objects across 20 categories, manipulated through 5 skills and over 100 tasks using 1,182 robot-object-skill combinations of MobileManiRL, which are further distributed across 100 scene placements. The dataset is split into 506 objects and 80 scenes for VLA training, plus 124 objects and 20 scenes for testing, yielding a total of 15,232 robot-object-skill-scene combinations for training and 920 combinations for testing. For each training combination, we generate 10 successful manipulation trajectories in Isaac Sim, resulting in 150K training trajectories. Each manipulation trajectory, $\mathcal{T} = \{L, (I_1, S_1, A_1), \dots, (I_t, S_t, A_t), \dots, (I_T, S_T, A_T)\}$, is recorded at 30 FPS with an average length of 160 frames, including one natural language instruction L ; synchronized 520×520 RGB, depth, and segmentation images I_t from both head-view and wrist-view cameras; the corresponding object and robot states S_t ; and the executed (6+D) dimensional action A_t at each timestep t . All states and actions are recorded in the global world coordinate frame.

4.3. MobileManiVLA Training

The objective is to use the generated MobileManiDataset to train a universal vision-language-action model, MobileManiVLA, for each of the G1 robot and XHand robot. MobileManiVLA is capable of performing mobile-based robotic manipulation of diverse ground and tabletop objects across varying initial poses, and can generalize to both unseen objects and unseen scenes. Following the design of CogACT [23], we structure our MobileManiVLA into three components: the vision, language, and action modules.

Vision and Language Modules. The vision and language modules are initialized from a pretrained vision-language model, PaliGemma-2 [39]. The vision module processes multi-view image inputs, including two RGB images and two depth images captured from the head-view and wrist-view cameras (each reshaped to $224 \times 224 \times 3$). These images are encoded via a SigLIP vision encoder into dense visual embeddings. In parallel, a language instruction of the form “`<skill> <object>`” (such as “open faucet” or

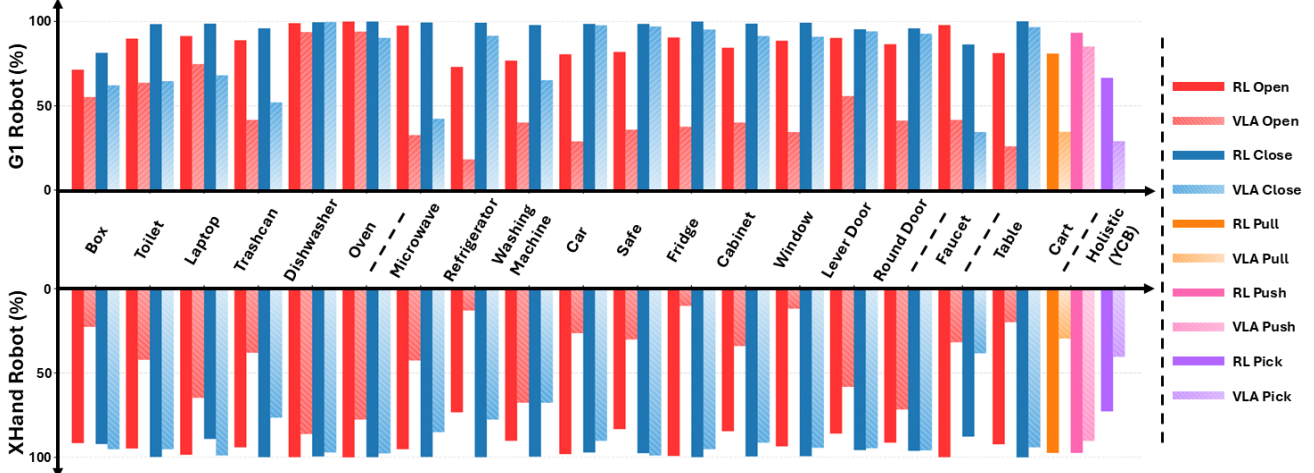


Figure 4. Success rates of MobileManiRL and MobileManiVLA on the G1 robot and XHand robot across 20 object categories and 5 mobile manipulation skills. In terms of manipulation motion patterns, objects like box, laptop, and oven require lid-flipping upward or downward; microwave, car, fridge, and round door require door-handle grasping followed by pivoting left or right; faucet requires handle rotation; table and cart require handle grasping with pulling or pushing; holistic (ycb) objects require object grasping and lifting.

“close door”) is tokenized and projected into language embeddings. The vision and language embeddings are then fused via a linear projection for alignment. Together with a learnable *cognition token* c , they are fed into a Gemma-2 language model [41] to produce an output feature f_t^c that captures both perceptual and instructional context.

Action Module with State Conditions. The action module is implemented as a diffusion-transformer (DiT) that takes as input: 1) a series of noisy actions $(a_t^i, a_{t+1}^i, \dots, a_{t+N}^i)$, where i denotes the current denoising step; 2) the encoded cognition feature f_t^c ; and 3) the state feature f_t^s , obtained by encoding the 6-d robot wrist pose using a lightweight MLP. Conditioned on f_t^c and f_t^s , the DiT iteratively predicts the clean actions $(a_t, a_{t+1}, \dots, a_{t+N})$ over multiple denoising steps, progressively refining its predictions toward physically consistent and goal-directed motions. All states and actions are expressed in the robot mobile base coordinate frame for consistency across scenes.

Training Objective and Inference Strategy. The vision, language, and action modules are trained end-to-end by minimizing the mean squared error (MSE) between the predicted and the ground truth noises, with the loss function:

$$\mathcal{L}_{\text{MSE}} = \mathbb{E}_{\epsilon \sim \mathcal{N}(0,1), i} \|\hat{\epsilon}^i - \epsilon\|_2, \quad (2)$$

where $\hat{\epsilon}^i$ is the predicted noise for the noisy action sequence $(a_t^i, a_{t+1}^i, \dots, a_{t+N}^i)$ at the i -th denoising step, and ϵ is the corresponding ground truth Gaussian noise.

During inference, MobileManiVLA predicts a chunk of actions with length $N = 16$ conditioned on the current instruction and observations. we adopt the adaptive ensemble strategy proposed in CogACT [23] to improve trajectory smoothness and robustness, with a window size of $K = 4$.

5. Experiment

For each of the G1 robot and XHand robot, we first train MobileManiRL on each of the 1,182 robot-object-skill combinations, with 1,024 simulation environments, a learning rate of $1e^{-3}$, and 4K iterations. Training is conducted in parallel on 32 NVIDIA V100 GPUs and requires about 4 days per robot. We then collect 15,232 robot-object-skill-scene combinations for training and 920 combinations for testing to generate the MobileManiDataset, resulting in 150K training trajectories. Trajectory generation is conducted in parallel on 8 NVIDIA RTX A6000 GPUs and requires about 6 days per robot. Finally, We train the MobileManiVLA model on MobileManiDataset, with a batch size of 480, a learning rate of $2e^{-5}$, and 320K iterations. Training is conducted on 8 NVIDIA B200 GPUs and takes about 12 days per robot.

5.1. Main Results

Figure 4 demonstrates the success rates of MobileManiRL and MobileManiVLA across the 20 object categories, while Table 3 summarizes the mean success rates over the 5 mobile manipulation skills. MobileManiRL is evaluated on seen objects with 1024 episodes per robot-object-skill combination, whereas MobileManiVLA is evaluated on unseen objects and scenes, with 10 episodes per robot-object-skill-scene combination. Both experiments are conducted with randomized robot initial poses to assess robustness.

Takeaway 1 — Object structure and skill complexity drive performance variance. For both MobileManiRL and MobileManiVLA, object categories like toilet, laptop, and dishwasher achieve higher success rates due to their relatively simple structures and motion patterns, typically involving lid-flipping without requiring complex han-

Skill	MobileManiRL (%)		MobileManiVLA (%)	
	G1 Robot	XHand Robot	G1 Robot	XHand Robot
Open	86.6	91.9	42.9	34.5
Close	96.2	96.5	75.8	77.5
Pull	80.8	97.3	34.4	29.4
Push	93.1	97.2	85.1	90.0
Pick	66.4	72.6	28.8	40.2
Mean	89.6	92.9	56.7	57.3

Table 3. Success rates of MobileManiRL and MobileManiVLA on the G1 robot and XHand robot across 5 manipulation skills.

dle grasping. In contrast, object categories such as car, door, and table present greater challenges, as they demand precise handle localization and stable grasp control. Regarding the mobile manipulation skills, open, pull, and pick, which require accurate and stable grasping of the object, are generally more difficult to learn than close and push.

Takeaway 2 — Generalization remains challenging for VLA models with the implicit inputs. Compared with MobileManiRL, the success rates of MobileManiVLA exhibit a moderate decline for two primary reasons. First, MobileManiRL is trained and evaluated individually on each seen robot-object-skill combination, whereas MobileManiVLA is trained as a universal model and evaluated on unseen objects and unseen scenes, which increases diversity and generalization difficulty. Second, MobileManiRL leverages explicit state-based observations, such as the world positions of the robot gripper/hand points, the object grasp and goal points, providing precise geometric information. In contrast, MobileManiVLA relies solely on implicit sensory inputs, including a language instruction, multi-view RGB-D images, and the robot wrist pose represented in the mobile base coordinate frame. This transition from explicit to implicit observations introduces additional learning challenges but enables MobileManiVLA to generalize effectively to unseen objects and unseen scenes in both simulation and the real world. The real world inference of MobileManiVLA is demonstrated in the Appendix.

Takeaway 3 — Dexterous hands improve manipulation precision and versatility. As shown in Table 3, with the MobileManiRL, the XHand robot achieves a higher success rate of **92.9%**, compared to **89.6%** for the G1 robot, highlighting the advantages of dexterous manipulation, particularly on the open, pull, and pick skills. While with MobileManiVLA, the G1 robot and XHand robot achieve comparable success rates of **56.7%** and **57.3%**, respectively. In this setting, the XHand robot performs worse on the open and pull skills, where its dexterous fingers often collide with surrounding object surfaces, preventing stable handle grasps. Such disturbance between the object body

(e.g., door faces) and the dexterous fingers significantly degrades the VLA performance. Nevertheless, with MobileManiVLA, the XHand robot outperforms the G1 robot on the pick skill, where the dexterous fingers can easily establish the force-closure grasps on the holistic objects.

5.2. Ablation Studies and Model Comparisons

We conduct ablation studies and model comparisons on a subset of MobileManiDataset that includes only the challenging skills: open, pull, and pick for the G1 robot, covering 272 training and 66 testing objects across 6 categories: laptop, cabinet, faucet, table, cart and holistic objects, providing 4,352 robot-object-skill-scene combinations for training and 264 unseen combinations for testing. All VLA models are trained with a batch size of 120 and 160K iterations, which are evaluated on unseen objects and scenes with 10 episodes per combination.

Takeaway 4 — Multi-view and multi-modality visual inputs significantly enhance policy generalization. Table 4 shows the success rates of MobileManiVLA with different image inputs. Using only the head-view RGB image yields a success rate of only 7.9%, indicating that a single global view is insufficient for precise manipulation in mobile-based settings. Adding either the head-view depth image or the wrist-view RGB image improves the performance to 14.1% and 14.9% respectively, suggesting that additional geometric or visual cues enhance spatial understanding. Finally, combining both RGB-D images from the head-view and wrist-view cameras achieves the highest success rate of 28.2%, confirming that multi-view and multi-modality visual inputs significantly enhance manipulation accuracy and generalization ability.

Takeaway 5 — State inputs from robot proprioception or simple object detection further improve performance. Table 4 reports the impact of different state inputs on the performance of MobileManiVLA. Compared with no state input, encoding the robot wrist pose in its mobile base coordinate frame increases the success rate from 22.4% to 28.2%, highlighting the importance of proprioceptive information for precise manipulation. Further incorporating the pseudo-observations, such as the first-frame positions of the object grasp point and goal point expressed in the robot mobile base coordinate frame, leads to additional performance gains, confirming that even coarse spatial priors about the object can enhance policy grounding and performance.

Takeaway 6 — Unseen objects present greater challenges than unseen scenes. Table 5 indicates the success rates of MobileManiVLA on seen or unseen objects and scenes. The model achieves the highest success rate of 59.6% when both objects and scenes are seen during testing. When evaluated with seen objects in unseen scenes or unseen objects in seen scenes, the success rates drop to 51.3% and 39.2% respectively, indicating that generalizing

Image Inputs				State Inputs			Success Rate (%)
Head RGB	Head Depth	Wrist RGB	Wrist Depth	Wrist Pose	Grasp Point	Goal Point	
✓				✓			7.9
✓	✓			✓			14.1
✓		✓		✓			14.9
✓	✓	✓	✓	✓			28.2
✓	✓	✓	✓				22.4
✓	✓	✓	✓	✓	✓		32.3
✓	✓	✓	✓	✓	✓	✓	36.6

Table 4. Ablation studies of MobileManiVLA on the G1 robot with different image inputs (top rows) and state inputs (bottom rows).

Unseen Object	Unseen Scene	Seen Object	Seen Scene	Success Rate (%)
		✓	✓	59.6
	✓	✓		51.3
✓			✓	39.2
✓	✓			28.2

Table 5. Ablation studies of MobileManiVLA on the G1 robot with seen or unseen objects and scenes.

Model	Success Rate (%)
OpenVLA [21] (7B)	4.5
CogACT [23] (7B)	6.8
π_0 [5] (3B)	11.2
$\pi_{0.5}$ [17] (3B)	18.8
MobileManiVLA (3B)	28.2

Table 6. Model comparisons of representative VLA models with their default architectures and input modalities on the G1 robot.

Fixed Base	Mobile Base	Success Rate (%)
	✓	82.8
✓		25.4

Table 7. Success rates of MobileManiRL on the G1 robot with fixed base or mobile base.

to unseen object structures presents greater challenges than adapting to new scene layouts. The lowest success rate of 28.2% occurs when both objects and scenes are unseen, reflecting the compounded difficulty of transferring manipulation skills to entirely novel environments.

Takeaway 7 — MobileManiBench provides a unified platform for training and evaluating VLA models. By offering standardized training and evaluation protocols across diverse robots, objects, tasks, scenes and input modalities, MobileManiBench enables consistent benchmarking of existing VLA models with their default architectures and inputs, as shown in Table 6. OpenVLA and CogACT receive only head-view RGB image, resulting in low success rates of 4.5% and 6.8%, respectively. π_0 and

$\pi_{0.5}$ process both head-view and wrist-view RGB images together with wrist pose states, achieving improved success rates of 11.2% and 18.8%, respectively. The stronger performance of $\pi_{0.5}$ arises from its pretraining on more mobile manipulation trajectories. Overall, MobileManiVLA achieves the highest success rate of 28.2% by jointly leveraging head-view and wrist-view RGB-D images along with wrist pose states, highlighting the advantages of multi-view and multi-modality inputs.

Takeaway 8 — Base mobility is crucial for effective manipulation beyond tabletop tasks. To evaluate the importance of base mobility during manipulation, we fix the G1 robot base and initialize it closer to the object grasp point than before (0.5m to 1.0m along the x and y axes). We train MobileManiRL under this fixed-base setting on several robot-object-skill combinations, including open laptop, open cabinet, open faucet, open table, pull cart and pick holistic (YCB) objects. As shown in Table 7, the success rates of MobileManiRL drop drastically when the robot base is fixed, confirming that base mobility is essential for spatial manipulation beyond static tabletop interactions.

6. Conclusion

We introduce MobileManiBench, a large-scale simulation-based benchmark designed to simplify model verification for mobile-based robotic manipulation. MobileManiBench encompasses 2 mobile-based robots with either parallel grippers or dexterous hands, 630 objects spanning 20 categories, and 5 mobile manipulation skills across 100+ tasks. By training a universal MobileManiRL policy on each robot-object-skill triplet, the benchmark autonomously generates the MobileManiDataset in 100 realistic scenes, which contains 300K trajectories with 3 data modalities: language instructions, multi-view RGB-depth-segmentation images, synchronized object/robot states and actions. Experiments demonstrate that MobileManiBench serves as a unified and scalable platform for developing and evaluating next-generation vision–language–action models, accelerating research toward general-purpose, embodied intelligence.

References

[1] AgiBot-World-Contributors, Qingwen Bu, Jisong Cai, Li Chen, Xiuqi Cui, Yan Ding, Siyuan Feng, Shenyuan Gao, Xindong He, Xuan Hu, Xu Huang, Shu Jiang, Yuxin Jiang, Cheng Jing, Hongyang Li, Jialu Li, Chiming Liu, Yi Liu, Yuxiang Lu, Jianlan Luo, Ping Luo, Yao Mu, Yuehan Niu, Yixuan Pan, Jiangmiao Pang, Yu Qiao, Guanghui Ren, Cheng Ruan, Jiaqi Shan, Yongjian Shen, Chengshi Shi, Mingkang Shi, Modi Shi, Chonghao Sima, Jianheng Song, Huijie Wang, Wenhao Wang, Dafeng Wei, Chengen Xie, Guo Xu, Junchi Yan, Cunbiao Yang, Lei Yang, Shukai Yang, Maoqing Yao, Jia Zeng, Chi Zhang, Qinglin Zhang, Bin Zhao, Chengyue Zhao, Jiaqi Zhao, and Jianchao Zhu. Agi-
bot world colosseo: A large-scale manipulation platform for scalable and intelligent embodied systems, 2025. 2, 3

[2] Chen Bao, Helin Xu, Yuzhe Qin, and Xiaolong Wang. Dexart: Benchmarking generalizable dexterous manipulation with articulated objects, 2023. 2, 3

[3] Lucas Beyer, Andreas Steiner, André Susano Pinto, Alexander Kolesnikov, Xiao Wang, Daniel Salz, Maxim Neumann, Ibrahim Alabdulmohsin, Michael Tschannen, Emanuele Bugliarello, et al. Paligemma: A versatile 3b vlm for transfer. *arXiv preprint arXiv:2407.07726*, 2024. 3

[4] Johan Bjorck, Fernando Castañeda, Nikita Cherniadev, Xingye Da, Runyu Ding, Linxi Fan, Yu Fang, Dieter Fox, Fengyuan Hu, Spencer Huang, et al. Gr0ot n1: An open foundation model for generalist humanoid robots. *arXiv preprint arXiv:2503.14734*, 2025. 2, 3

[5] Kevin Black, Noah Brown, Danny Driess, Adnan Esmail, Michael Equi, Chelsea Finn, Niccolò Fusai, Lachy Groom, Karol Hausman, Brian Ichter, et al. π_0 : A vision-language-action flow model for general robot control. *arXiv:2410.24164*, 2024. 2, 3, 8

[6] Anthony Brohan, Noah Brown, Justice Carbajal, Yevgen Chebotar, Joseph Dabis, Chelsea Finn, Keerthana Gopalakrishnan, Karol Hausman, Alex Herzog, Jasmine Hsu, et al. RT-1: Robotics transformer for real-world control at scale. *arXiv:2212.06817*, 2022. 2, 3

[7] Berk Calli, Arjun Singh, Aaron Walsman, Siddhartha S. Srinivasa, Pieter Abbeel, and Aaron M. Dollar. The ycb object and model set: Towards common benchmarks for manipulation research. In *Proceedings of the IEEE International Conference on Advanced Robotics (ICAR)*, pages 510–517, 2015. 4, 12

[8] Chilam Cheang, Sijin Chen, Zhongren Cui, Yingdong Hu, Liqun Huang, Tao Kong, Hang Li, Yifeng Li, Yuxiao Liu, Xiao Ma, et al. Gr-3 technical report. *arXiv preprint arXiv:2507.15493*, 2025. 2, 3

[9] Junting Chen, Haotian Liang, Lingxiao Du, Weiyun Wang, Mengkang Hu, Yao Mu, Wenhui Wang, Jifeng Dai, Ping Luo, Wenqi Shao, and Lin Shao. Owmm-agent: Open world mobile manipulation with multi-modal agentic data synthesis, 2025. 2, 3

[10] Tianxing Chen, Zanxin Chen, Baijun Chen, Zijian Cai, Yibin Liu, Zixuan Li, Qiwei Liang, Xianliang Lin, Yiheng Ge, Zhenyu Gu, Weiliang Deng, Yubin Guo, Tian Nian, Xuanbing Xie, Qiangyu Chen, Kailun Su, Tianling Xu, Guodong Liu, Mengkang Hu, Huan ang Gao, Kaixuan Wang, Zhixuan Liang, Yusen Qin, Xiaokang Yang, Ping Luo, and Yao Mu. Robotwin 2.0: A scalable data generator and benchmark with strong domain randomization for robust bimanual robotic manipulation, 2025. 2, 3

[11] Xi Chen, Josip Djolonga, Piotr Padlewski, Basil Mustafa, Soravit Changpinyo, Jialin Wu, Carlos Riquelme Ruiz, Sebastian Goodman, Xiao Wang, Yi Tay, et al. Pali-x: On scaling up a multilingual vision and language model. *arXiv preprint arXiv:2305.18565*, 2023. 3

[12] NVIDIA Corporation. Isaac lab, 2023. Accessed: 2025-11-18. 12

[13] Danny Driess, Fei Xia, Mehdi SM Sajjadi, Corey Lynch, Aakanksha Chowdhery, Ayzaan Wahid, Jonathan Tompson, Quan Vuong, Tianhe Yu, Wenlong Huang, et al. Palm-e: An embodied multimodal language model. 2023. 3

[14] Zipeng Fu, Tony Z. Zhao, and Chelsea Finn. Mobile aloha: Learning bimanual mobile manipulation with low-cost whole-body teleoperation, 2024. 2, 3

[15] Jiayuan Gu, Fanbo Xiang, Xuanlin Li, Zhan Ling, Xiqiang Liu, Tongzhou Mu, Yihe Tang, Stone Tao, Xinyue Wei, Yunchao Yao, Xiaodi Yuan, Pengwei Xie, Zhiao Huang, Rui Chen, and Hao Su. Maniskill2: A unified benchmark for generalizable manipulation skills, 2023. 2, 3

[16] Wenlong Huang, Chen Wang, Yunzhu Li, Ruohan Zhang, and Li Fei-Fei. Rekep: Spatio-temporal reasoning of relational keypoint constraints for robotic manipulation, 2024. 4

[17] Physical Intelligence, Kevin Black, Noah Brown, James Darpinian, Karan Dhabalia, Danny Driess, Adnan Esmail, Michael Equi, Chelsea Finn, Niccolò Fusai, et al. $\pi_{0.5}$: a vision-language-action model with open-world generalization. *arXiv:2504.16054*, 2025. 2, 3, 8

[18] Stephen James, Zicong Ma, David Rovick Arrojo, and Andrew J. Davison. Rlbench: The robot learning benchmark & learning environment, 2019. 2, 3

[19] Siddharth Karamcheti, Suraj Nair, Ashwin Balakrishna, Percy Liang, Thomas Kollar, and Dorsa Sadigh. Prismatic vlms: Investigating the design space of visually-conditioned language models. In *Forty-first International Conference on Machine Learning*, 2024. 3

[20] Alexander Khazatsky, Karl Pertsch, Suraj Nair, Ashwin Balakrishna, Sudeep Dasari, Siddharth Karamcheti, Soroush Nasiriany, Mohan Kumar Srirama, Lawrence Yunliang Chen, Kirsty Ellis, Peter David Fagan, Joey Hejna, Masha Itkina, Marion Lepert, Yecheng Jason Ma, Patrick Tree Miller, Jimmy Wu, Suneel Belkhale, Shivin Dass, Huy Ha, Arhan Jain, Abraham Lee, Youngwoon Lee, Marius Memmel, Sungjae Park, Ilija Radosavovic, Kaiyuan Wang, Albert Zhan, Kevin Black, Cheng Chi, Kyle Beltran Hatch, Shan Lin, Jingpei Lu, Jean Mercat, Abdul Rehman, Pannag R Sanketi, Archit Sharma, Cody Simpson, Quan Vuong, Homer Rich Walke, Blake Wulfe, Ted Xiao, Jonathan Heewon Yang, Arefeh Yavary, Tony Z. Zhao, Christopher Agia, Rohan Baijal, Mateo Guaman Castro, Daphne Chen, Qiuyu Chen, Trinity Chung, Jaimyn Drake, Ethan Paul Foster, Jensen Gao, Vitor Guizilini, David Antonio Herrera,

Minho Heo, Kyle Hsu, Jiaheng Hu, Muhammad Zubair Irshad, Donovan Jackson, Charlotte Le, Yunshuang Li, Kevin Lin, Roy Lin, Zehan Ma, Abhiram Maddukuri, Suvir Mirchandani, Daniel Morton, Tony Nguyen, Abigail O'Neill, Rosario Scalise, Derick Seale, Victor Son, Stephen Tian, Emi Tran, Andrew E. Wang, Yilin Wu, Annie Xie, Jingyun Yang, Patrick Yin, Yunchu Zhang, Osbert Bastani, Glen Berseth, Jeannette Bohg, Ken Goldberg, Abhinav Gupta, Abhishek Gupta, Dinesh Jayaraman, Joseph J Lim, Jitendra Malik, Roberto Martín-Martín, Subramanian Ramamoorthy, Dorsa Sadigh, Shuran Song, Jiajun Wu, Michael C. Yip, Yuke Zhu, Thomas Kollar, Sergey Levine, and Chelsea Finn. Droid: A large-scale in-the-wild robot manipulation dataset, 2025. 2, 3

[21] Moo Jin Kim, Karl Pertsch, Siddharth Karamchetti, Ted Xiao, Ashwin Balakrishna, Suraj Nair, Rafael Rafailov, Ethan Foster, Grace Lam, Pannag Sanketi, et al. OpenVLA: An open-source vision-language-action model. *arXiv:2406.09246*, 2024. 2, 8

[22] Moo Jin Kim, Chelsea Finn, and Percy Liang. Fine-tuning vision-language-action models: Optimizing speed and success. *arXiv:2502.19645*, 2025. 2, 3

[23] Qixiu Li, Yaobo Liang, Zeyu Wang, Lin Luo, Xi Chen, Mozheng Liao, Fangyun Wei, Yu Deng, Sicheng Xu, Yizhong Zhang, et al. CogACT: A foundational vision-language-action model for synergizing cognition and action in robotic manipulation. *arXiv:2411.19650*, 2024. 2, 3, 5, 6, 8

[24] Qixiu Li, Yu Deng, Yaobo Liang, Lin Luo, Lei Zhou, Chengtang Yao, Lingqi Zeng, Zhiyuan Feng, Huizhi Liang, Sicheng Xu, et al. Scalable vision-language-action model pretraining for robotic manipulation with real-life human activity videos. *arXiv preprint arXiv:2510.21571*, 2025.

[25] Xinghang Li, Minghuan Liu, Hanbo Zhang, Cunjun Yu, Jie Xu, Hongtao Wu, Chilam Cheang, Ya Jing, Weinan Zhang, Huaping Liu, et al. Vision-language foundation models as effective robot imitators. In *ICLR*, 2022. 2, 3

[26] Xuanlin Li, Kyle Hsu, Jiayuan Gu, Karl Pertsch, Oier Mees, Homer Rich Walke, Chuyuan Fu, Ishikaa Lunawat, Isabel Sieh, Sean Kirmani, Sergey Levine, Jiajun Wu, Chelsea Finn, Hao Su, Quan Vuong, and Ted Xiao. Evaluating real-world robot manipulation policies in simulation. *arXiv preprint arXiv:2405.05941*, 2024. 3

[27] Yu Li, Xiaojie Zhang, Ruihai Wu, Zilong Zhang, Yiran Geng, Hao Dong, and Zhaofeng He. Unidoormanip: Learning universal door manipulation policy over large-scale and diverse door manipulation environments, 2024. 2, 3, 4, 12

[28] Bo Liu, Yifeng Zhu, Chongkai Gao, Yihao Feng, Qiang Liu, Yuke Zhu, and Peter Stone. Libero: Benchmarking knowledge transfer for lifelong robot learning, 2023. 3

[29] Haotian Liu, Chunyuan Li, Qingyang Wu, and Yong Jae Lee. Visual instruction tuning. *NeurIPS*, 2023. 3

[30] Songming Liu, Lingxuan Wu, Bangguo Li, Hengkai Tan, Huayu Chen, Zhengyi Wang, Ke Xu, Hang Su, and Jun Zhu. RDT-1B: A diffusion foundation model for bimanual manipulation. *ICLR*, 2025. 2, 3

[31] Oier Mees, Lukas Hermann, Erick Rosete-Beas, and Wolfram Burgard. Calvin: A benchmark for language-conditioned policy learning for long-horizon robot manipulation tasks, 2022. 3

[32] Soroush Nasiriany, Abhiram Maddukuri, Lance Zhang, Adeet Parikh, Aaron Lo, Abhishek Joshi, Ajay Mandlekar, and Yuke Zhu. Robocasa: Large-scale simulation of everyday tasks for generalist robots, 2024. 2, 3

[33] NVIDIA. Isaac Sim. 2, 3, 5, 12, 14

[34] Abby O'Neill, Abdul Rehman, Abhiram Maddukuri, Abhishek Gupta, Abhishek Padalkar, Abraham Lee, Acorn Pooley, Agrim Gupta, Ajay Mandlekar, et al. Open X-Embodiment: Robotic learning datasets and RT-X models. In *ICRA*, 2024. 2, 3

[35] Delin Qu, Haoming Song, Qizhi Chen, Yuanqi Yao, Xinyi Ye, Yan Ding, Zhigang Wang, JiaYuan Gu, Bin Zhao, et al. SpatialVLA: Exploring spatial representations for visual-language-action model. *arXiv:2501.15830*, 2025. 2, 3

[36] Robotera. Xhand, 2025. <https://www.robotera.com/en/>. 3, 12

[37] John Schulman, Filip Wolski, Prafulla Dhariwal, Alec Radford, and Oleg Klimov. Proximal policy optimization algorithms, 2017. 2, 12

[38] Hao Shi, Bin Xie, Yingfei Liu, Lin Sun, Fengrong Liu, Tiancai Wang, Erjin Zhou, Haoqiang Fan, Xiangyu Zhang, and Gao Huang. Memoryvla: Perceptual-cognitive memory in vision-language-action models for robotic manipulation. *arXiv preprint arXiv:2508.19236*, 2025. 2, 3

[39] Andreas Steiner, André Susano Pinto, Michael Tschannen, Daniel Keysers, Xiao Wang, Yonatan Bitton, Alexey Gritsenko, Matthias Minderer, Anthony Sherbondy, Shangbang Long, et al. Paligemma 2: A family of versatile vlms for transfer. *arXiv preprint arXiv:2412.03555*, 2024. 5

[40] Gemini Team, Rohan Anil, Sebastian Borgeaud, Jean-Baptiste Alayrac, Jiahui Yu, Radu Soricut, Johan Schalkwyk, Andrew M Dai, Anja Hauth, Katie Millican, et al. Gemini: a family of highly capable multimodal models. *arXiv:2312.11805*, 2023. 3

[41] Gemma Team, Morgane Riviere, Shreya Pathak, Pier Giuseppe Sessa, Cassidy Hardin, Surya Bhupatiraju, Léonard Hussonot, Thomas Mesnard, Bobak Shahriari, Alexandre Ramé, et al. Gemma 2: Improving open language models at a practical size. *arXiv preprint arXiv:2408.00118*, 2024. 6

[42] Gemini Robotics Team, Saminda Abeyruwan, Joshua Ainslie, Jean-Baptiste Alayrac, Montserrat Gonzalez Arenas, Travis Armstrong, Ashwin Balakrishna, Robert Baruch, Maria Bauza, Michiel Blokzijl, et al. Gemini robotics: Bringing ai into the physical world. *arXiv preprint arXiv:2503.20020*, 2025. 2, 3

[43] Genie Sim Team. Genie sim assets. https://github.com/AgibotTech/genie_sim, 2025. 5, 12, 14

[44] Octo Model Team, Dibya Ghosh, Homer Walke, Karl Pertsch, Kevin Black, Oier Mees, Sudeep Dasari, Joey Hejna, Tobias Kreiman, Charles Xu, et al. Octo: An open-source generalist robot policy. *arXiv:2405.12213*, 2024. 2, 3

[45] Hanqing Wang, Jiahe Chen, Wensi Huang, Qingwei Ben, Tai Wang, Boyu Mi, Tao Huang, Siheng Zhao, Yilun Chen,

Sizhe Yang, Peizhou Cao, Wenye Yu, Zichao Ye, Jialun Li, Junfeng Long, Zirui Wang, Huiling Wang, Ying Zhao, Zhongying Tu, Yu Qiao, Dahua Lin, and Jiangmiao Pang. Grutopia: Dream general robots in a city at scale, 2024. 3

[46] Wenbo Wang, Gen Li, Miguel Zamora, and Stelian Coros. Trtm: Template-based reconstruction and target-oriented manipulation of crumpled cloths, 2024. 2

[47] Wenbo Wang, Fangyun Wei, Lei Zhou, Xi Chen, Lin Luo, Xiaohan Yi, Yizhong Zhang, Yaobo Liang, Chang Xu, Yan Lu, Jiaolong Yang, and Baining Guo. Unigraspttransformer: Simplified policy distillation for scalable dexterous robotic grasping, 2025. 3

[48] Yuqi Wang, Xinghang Li, Wenxuan Wang, Junbo Zhang, Yingyan Li, Yuntao Chen, Xinlong Wang, and Zhaoxiang Zhang. Unified vision-language-action model. *arXiv:2506.19850*, 2025. 2, 3

[49] Junjie Wen, Yichen Zhu, Jinning Li, Zhibin Tang, Chaomin Shen, and Feifei Feng. DexVLA: Vision-language model with plug-in diffusion expert for general robot control. In *CoRL*, 2025. 2, 3

[50] Fan Xiang, Kaichun Mo, Ye Xia, Hao Liu, Fangyin Zhang, Liang Han, Leonidas J. Guibas, Jingwei Xiao, Hao Dong, Ye Yuan, et al. Partnet-mobility: A large-scale database for articulated objects. *Proceedings of the IEEE/CVF Conference on Computer Vision and Pattern Recognition (CVPR)*, pages 11359–11368, 2020. 4, 12

[51] Jianwei Yang, Reuben Tan, Qianhui Wu, Ruijie Zheng, Baolin Peng, Yongyuan Liang, Yu Gu, Mu Cai, Seonghyeon Ye, Joel Jang, et al. Magma: A foundation model for multi-modal ai agents. In *Proceedings of the Computer Vision and Pattern Recognition Conference*, pages 14203–14214, 2025. 2, 3

[52] Hui Zhang, Sammy Christen, Zicong Fan, Otmar Hilliges, and Jie Song. GraspXL: Generating grasping motions for diverse objects at scale. In *European Conference on Computer Vision (ECCV)*, 2024. 4

[53] Shiduo Zhang, Zhe Xu, Peiju Liu, Xiaopeng Yu, Yuan Li, Qinghui Gao, Zhaoye Fei, Zhangyue Yin, Zuxuan Wu, Yu-Gang Jiang, and Xipeng Qiu. Vlabench: A large-scale benchmark for language-conditioned robotics manipulation with long-horizon reasoning tasks, 2024. 2, 3

[54] Wenyao Zhang, Hongsi Liu, Zekun Qi, Yunnan Wang, Xinqiang Yu, Jiazhao Zhang, Runpei Dong, Jiawei He, Fan Lu, He Wang, et al. Dreamvla: a vision-language-action model dreamed with comprehensive world knowledge. *arXiv preprint arXiv:2507.04447*, 2025. 2, 3

[55] Zhenyu Zhao, Hongyi Jing, Xiawei Liu, Jiageng Mao, Abha Jha, Hanwen Yang, Rong Xue, Sergey Zakharov, Vitor Guizilini, and Yue Wang. Humanoid everyday: A comprehensive robotic dataset for open-world humanoid manipulation, 2025. 2, 3

[56] Jinliang Zheng, Jianxiong Li, Zhihao Wang, Dongxiu Liu, Xirui Kang, Yuchun Feng, Yinan Zheng, Jiayin Zou, Yilun Chen, Jia Zeng, et al. X-vla: Soft-prompted transformer as scalable cross-embodiment vision-language-action model. *arXiv preprint arXiv:2510.10274*, 2025. 3

[57] Yifan Zhong, Xuchuan Huang, Ruochong Li, Ceyao Zhang, Zhang Chen, Tianrui Guan, Fanlian Zeng, Ka Num Lui, et al. DexGraspVLA: A vision-language-action framework towards general dexterous grasping. *arXiv:2502.20900*, 2025. 2, 3

[58] Yuke Zhu, Josiah Wong, Ajay Mandlekar, Roberto Martín-Martín, Abhishek Joshi, Kevin Lin, Abhiram Maddukuri, Soroush Nasiriany, and Yifeng Zhu. robosuite: A modular simulation framework and benchmark for robot learning. In *arXiv preprint arXiv:2009.12293*, 2020. 3

[59] Brianna Zitkovich, Tianhe Yu, Sichun Xu, Peng Xu, Ted Xiao, Fei Xia, Jialin Wu, Paul Wohlhart, Stefan Welker, Ayzaan Wahid, et al. RT-2: Vision-language-action models transfer web knowledge to robotic control. In *CoRL*, 2023. 2, 3

MobileManiBench: Simplifying Model Verification for Mobile Manipulation

Supplementary Material

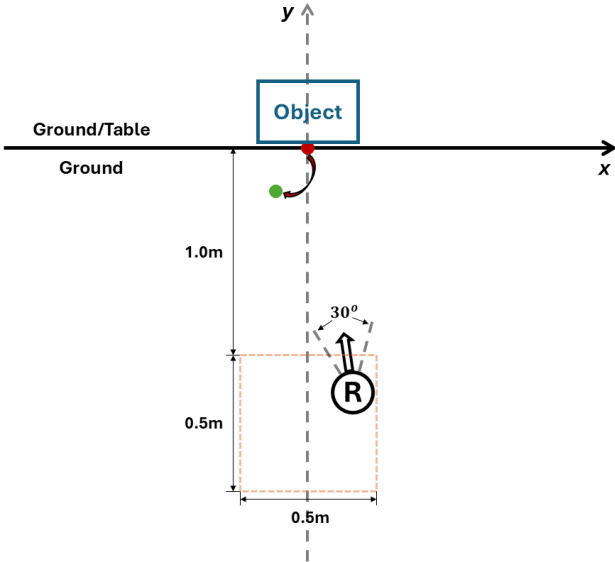


Figure 5. Initialization of the robot, object, ground, and table.

A. Implementation Details

A.1. Digital Assets

MobileManiBench utilizes NVIDIA Isaac Sim 4.5 [33] as the simulation platform and employs NVIDIA Isaac Lab [12] to construct the simulation environments. All policies operate at 30 FPS, while the simulation runs at 60 FPS.

Robot Assets. MobileManiBench encompasses 2 digital robots: the G1 robot from AGIBOT [?] and the XHand robot from RobotEra [36]. The USD files for these robots are created by processing their original URDF files and adding 2 degrees of freedom (DOFs) at their robot base: one rotational DOF around the z-axis and one translational DOF along the y-axis, as shown in Figure 1.

Object Assets. MobileManiBench includes 630 digital objects across 20 categories: box, toilet, laptop, trashcan, dishwasher, oven, microwave, refrigerator, washing machine, car, safe, fridge, cabinet, window, lever door, round door, faucet, table, cart, and holistic (YCB) objects, which are sourced from the PartNet-Mobility [50], UniDoorManip [27], and YCB [7] datasets. The USD files for these objects are constructed by processing their original URDF files. The object grasp points are automatically located by detecting the object "handle" body in their URDF files. For those lid-structured objects that lack a "handle" body, such as boxes, laptops, toilets, trashcans, and washing machines, we manually label the grasp points and initialize the lid as opened by 10 degrees for the open skill. For Holistic (YCB) objects, the center of mass is used as the grasp point.

Scene Assets. MobileManiBench features 100 realistic

scene placements for trajectory generation. It collects 6 scene assets from the Isaac Sim [33] and 4 scene assets from the Genie Sim [43], with each scene asset contains multiple rooms. MobileManiBench places the 20 categories of objects into 5 realistic scene settings for trajectory rendering: space (cart), wall (toilet, trashcan, refrigerator, washing machine, fridge, cabinet, table), door (window, lever door, round door), outdoor (car), and tabletop (box, laptop, dishwasher, oven, microwave, safe, faucet, holistic objects). For each scene setting, we manually annotate 20 scene placements within the scene assets, as shown in Figure 10 - 14.

A.2. Environment Setup

Initialization. Each environment contains one robot and one object placed either on the ground or on a tabletop with random heights ranging from 0.2 to 0.7 meters. The object's grasp point initialized to zero x and y coordinates, as shown in Figure 5. The robot is first initialized with the same pose, randomly within the orange zone, facing the object grasp point, and then rotating around the z axis from -15° to 15° . For the open skill, the goal points for articulated objects are set to the positions of their grasp points when the object is 60% open. For the close skill, the goal points are set as the positions of the grasp points when the object is closed, with the object initialized from 40% to 80% opened. For carts and holistic (YCB) objects, a target displacement and height of 0.2 meters are set for pull, push, and pick tasks.

Skill Definition. MobileManiBench designs 5 mobile manipulation skills: *open* and *close* for objects including boxes, toilets, laptops, trashcans, dishwashers, ovens, microwaves, refrigerators, washing machines, cars, safes, fridges, cabinets, windows, lever doors, round doors, faucets, and tables; *pull* and *push* for carts; and *pick* for holistic (YCB) objects. Each robot-object-skill combination is parameterized using keypoint-based displacements of the robot's gripper/hand points, the object grasp point, and the goal point. A manipulation is considered successful if the object grasp point reaches the goal point within a threshold of 5cm.

A.3. MobileManipRL Training

MobileManiBench trains a universal state-based MobileManipRL on each robot-object-skill pair. It utilizes PPO [37] as the optimization algorithm.

Action Space. Each robot is controlled with $(6+D)$ dimensional actions, where the first 6 dimensions represent the wrist pose displacement relative to the previous frame, from which inverse kinematics computes the target joint angles of mobile base (2-d) and right arm (7-d). The remaining D dimensions correspond to the target joint angles of end ef-

Input Type	Elements (Dimension)
Time (30)	Sine-cosine time embedding (30).
Object State (9)	Object grasp point position (3) and rotation (3); Object goal point position (3).
Robot Proprioception (78/135)	Robot palm position (3), rotation (3), linear velocity (3), and angular velocity (3); Robot fingertip positions (9/15), rotations (9/15), linear velocities (9/15), and angular velocities (9/15); Robot active joint angles (10/21), joint velocities (10/21) and joint accelerations (10/21).
Robot-Object Distance (22/31)	Robot palm to object grasp point distance (1); Robot fingertips to object grasp point distances (3/5); Robot active joints to object grasp point distances (15/22); Robot palm to object grasp point displacement (3).
Previous Action (7/18)	Previous target robot wrist position displacement (3) and rotation displacement (3); Previous target robot finger joint angles (1/12).

Table 8. Input types of MobileManiRL for the G1 robot and the XHand robot.

factor. This formulation yields 7-d actions for the G1 robot and 18-d actions for the XHand robot.

Observation Space. Table 8 summarizes the 5 input types used in MobileManiRL. Specifically, *Time* encodes the timestep embedding; *Object State* represents the states of the object grasp point and goal point; *Robot Proprioception* captures the robot’s body and joint states; *Robot-Object Distance* measures the distances between the robot gripper/hand points and the object grasp point; and *Previous Action* records the previous (6+D)-dimensional action.

Reward Function. The reward function described in Eq.(1) of the main paper comprises five components: R_d , R_a , R_g , R_m , and R_s . These reward components are governed by a grasp flag f_g , which indicates whether the gripper/hand has successfully grasped the object grasp point.

The distance reward R_d penalizes the average Chamfer Distance (CD) between the gripper/hand points P_{hand}^i and the object grasp point P_{grasp} , promoting contact and encouraging a secure grasp. It additionally penalizes the Chamfer Distance between the object grasp point P_{obj} and the goal point P_{goal} :

$$R_d = -\omega_d \left(\frac{1}{N} \sum_{i=1}^N CD(P_{hand}^i, P_{obj}) + CD(P_{goal}, P_{obj}) \right), \quad (3)$$

where the reward weight ω_d is set as 1.0, and N is the number of gripper/hand points, as shown in Figure 2.

The grasp flag f_g is set to 1 when the average Chamfer Distance between the gripper/hand points and the object grasp point falls below a predefined threshold $\lambda_c = 0.1$:

$$f_g = \mathbb{1} \left[\frac{1}{N} \sum_{i=1}^N CD(P_{hand}^i, P_{obj}) < \lambda_g \right], \quad (4)$$

where $\mathbb{1}[\cdot]$ denotes the indicator function.

Before the grasp is established, the approach action reward R_a penalizes deviations of the current action a from a

reference approach action a_{ref_a} :

$$R_a = -\omega_a \|a - a_{ref_a}\|_2, \quad (5)$$

where the reward weight ω_a is set as 0.2. The reference approach action a_{ref_a} consists of: (1) the displacement from the gripper/hand palm point P_{palm} to the object grasp point P_{obj} , (2) the displacement from the current palm rotation R_{palm} to the initial palm rotation R_{palm}^{init} , and (3) the initial joint angles for the end-effector joints:

$$\begin{aligned} a_{ref_a}[0 : 3] &= P_{obj} - P_{palm}, \\ a_{ref_a}[3 : 6] &= R_{palm}^{init} - R_{palm}, \\ a_{ref_a}[6 : 6 + D] &= \text{Joint}^{init}. \end{aligned} \quad (6)$$

This reference approach action encourages the gripper/hand to stay open while approaching the object grasp point.

Once a grasp is established, the rewards R_g , R_m , and R_s are introduced to guide the moving process. The grasp bonus R_g encourages the grasp with $\omega_g = 1.0$:

$$R_g = \omega_g, \quad (7)$$

The move action reward R_m penalizes deviations of the current action a from a reference move action a_{ref_m} :

$$R_m = -\omega_m \|a[0 : 3] - a_{ref_m}[0 : 3]\|_2, \quad (8)$$

$$a_{ref_m}[0 : 3] = P_{goal} - P_{palm} \quad (9)$$

where ω_m is set as 0.2. This reference move action encourages the gripper/hand to move to the goal point.

The success reward R_s provides a bonus when the object grasp point successfully reaches the goal point, defined by a threshold $\lambda_g = 0.05$:

$$R_s = \omega_s \mathbb{1}[\|P_{goal} - P_{obj}\|_2 < \lambda_g], \quad (10)$$

where ω_s is set as 2.0.

Object	Number			MobileManiRL (%)				MobileManiVLA (%)			
	Total	Train	Test	Open/Pull/Pick		Close/Push		Open/Pull/Pick		Close/Push	
				G1	XHand	G1	XHand	G1	XHand	G1	XHand
Box	14	10	4	71.2	91.4	81.2	92.0	55.0	22.5	61.9	95.0
Toilet	30	25	5	89.6	94.6	98.2	99.6	63.5	42.0	64.5	95.0
Laptop	36	30	6	91.2	98.4	98.5	88.9	74.6	64.6	67.9	98.8
Trashcan	36	30	6	88.7	93.9	95.8	99.8	41.4	37.9	51.8	76.4
Dishwasher	25	20	5	98.8	99.7	99.4	99.4	93.5	86.0	99.5	97.0
Oven	12	10	2	99.7	99.9	99.8	99.7	93.8	77.5	90.0	97.5
Microwave	5	3	2	97.4	95.0	99.2	99.6	32.5	42.5	42.2	85.0
Refrigerator	52	40	12	72.9	73.2	99.1	99.8	18.1	12.8	91.3	77.5
Washing Machine	12	10	2	76.6	90.0	97.7	99.5	40.0	67.5	65.0	67.5
Car	12	10	2	80.3	97.9	98.4	97.0	28.7	26.2	97.5	90.0
Safe	19	15	4	81.8	83.1	98.3	97.4	35.6	30.0	96.9	98.8
Fridge	10	8	2	90.4	99.1	99.7	99.7	37.5	10.0	95.0	95.0
Cabinet	22	20	2	84.2	84.4	98.5	99.4	40.0	33.8	91.2	91.2
Window	18	15	3	88.4	93.4	99.1	99.2	34.2	11.7	90.8	94.2
Lever Door	22	18	4	90.0	85.8	95.2	95.6	55.6	58.1	94.0	94.5
Round Door	25	20	5	86.3	91.1	95.7	96.0	41.0	71.5	92.5	95.7
Faucet	78	60	18	97.7	99.8	86.3	87.5	41.4	31.7	34.3	38.1
Table	108	90	18	81.0	92.2	99.9	99.9	25.8	19.7	96.4	93.9
Cart	16	12	4	80.8	97.3	93.1	97.2	34.4	29.4	85.0	90.0
Holistic (YCB)	78	60	18	66.4	72.6	-	-	28.8	40.2	-	-
Summary	630	506	124	83.9	89.7	96.2	96.5	40.3	36.5	75.8	81.5

Table 9. MobileManiBench object numbers and success rates of MobileManiRL and MobileManiVLA.

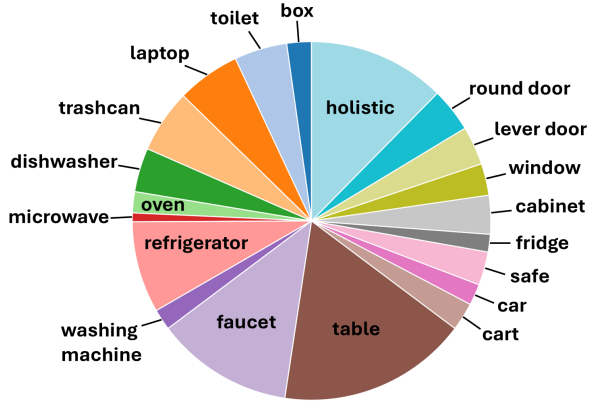


Figure 6. MobileManiBench object distribution.

A.4. MobileManiDataset Generation

MobileManiBench generates the MobileManiDataset by rendering MobileManiRL in diverse realistic scenes.

Realistic Scenes. We place the 20 categories of objects into 5 realistic scene settings for trajectory rendering: space, wall, door, tabletop, and outdoor. For each setting, we manually annotate 20 scene placements using digital assets from the Isaac Sim [33] and Genie Sim [43], yielding 80 for training and 20 for testing, as shown in Figure 10 - 14.

Dataset Analysis. MobileManiDataset comprises a total of 630 objects across 20 categories, as shown in Figure 6 and Table 9, which are manipulated through 5 skills and over 100 tasks using 1,182 robot-object-skill combinations of MobileManiRL. The dataset is split into 506 objects and 80 scenes for VLA training, plus 124 objects and 20 scenes for testing, yielding a total of 15,232 robot-object-skill-scene combinations for training and 920 combinations for testing. For each training combination, we generate 10 successful manipulation trajectories in Isaac Sim, resulting in 150K training trajectories. Each manipulation trajectory, $\mathcal{T} = \{L, (I_1, S_1, A_1), \dots, (I_t, S_t, A_t), \dots, (I_T, S_T, A_T)\}$, is recorded at 30 FPS with an average length of 160 frames, including one natural language instruction L of the form “<skill> <object>”; synchronized $520 \times 520 \times 3$ RGB, depth, and segmentation images I_t from both head-view and wrist-view cameras; the corresponding object and robot states S_t in Table 8; and the executed (6+D) dimensional action A_t at each timestep t . All states and actions are recorded in the global world coordinate frame. Each depth image is obtained by first clipping the raw depth values to 0–5 meters and subsequently normalized to pixel values between 0 and 255. Manipulation trajectories for the G1 robot and the XHand robot are shown in Figure 15 - 19.

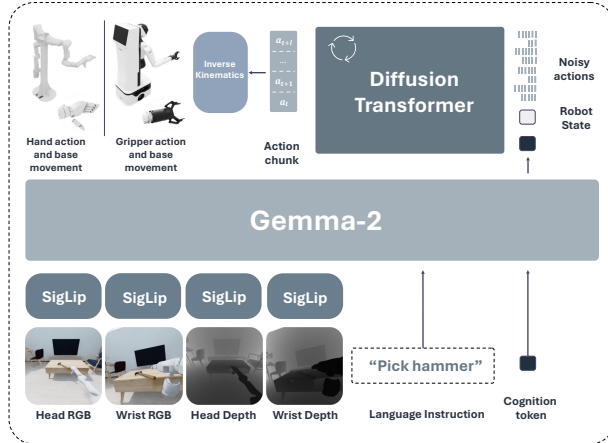


Figure 7. Model architecture of MobileManiVLA.

A.5. MobileManiVLA

Figure 7 illustrates the model architecture of MobileManiVLA, which is discussed in detail in Section 4.3. Our framework incorporates multiple modalities as inputs, including multi-view RGB images, multi-view depth images, language instructions, and robot state information. The multi-view RGB and multi-view depth images are each passed through a single SigLIP encoder to obtain their respective embeddings. These embeddings are then projected into the same representation space as the language embeddings and concatenated together, along with the language tokens and a cognition token. Then they are fed into the Gemma-2 language model.

The final-layer embedding of the cognition token produced by Gemma-2, together with the robot state, serves as the conditioning for the diffusion model. This conditioning, combined with a noisy action chunk, is processed by a DiT-Base model (about 90M parameters). Through a 10-step DDIM denoising procedure, the model iteratively generates clean delta end-effector poses and gripper/hand actions, from which inverse kinematics computes the target joint angles of mobile base and right arm.

B. Experiment Details

B.1. Main Results

For each of the G1 robot and XHand robot, we first train MobileManiRL on each of the 1,182 robot-object-skill combinations, which provide 15,232 robot-object-skill-scene combinations for VLA training and 920 combinations for VLA testing when generating the MobileManiDataset, yielding 150K training trajectories for MobileManiVLA training. Table 9 demonstrates the detailed success rates of MobileManiRL and MobileManiVLA across the 20 object categories. MobileManiRL is evaluated on seen objects with 1024 episodes per robot-object-skill combination,

Object	Multi-view RGB-D	Multi-view RGB	Head-view RGB-D	Head-view RGB
Laptop	72.5	40.8	30.0	16.9
Cabinet	22.3	13.8	12.5	6.8
Faucet	30.6	12.0	12.7	8.3
Table	19.3	13.4	8.9	7.1
Cart	23.5	13.8	9.4	6.3
Holistic	21.7	11.2	16.7	5.9
Mean	28.2	14.9	14.1	7.9

Table 10. Success rates of MobileManiVLA on the G1 Robot with different image inputs.

Object	None	Hand Pose	+ Grasp Point	+ Goal Point
Laptop	59.4	72.5	83.3	85.4
Cabinet	18.8	22.3	23.8	32.5
Faucet	27.1	30.6	36.4	40.4
Table	12.5	19.3	20.7	24.8
Cart	28.1	23.5	25.0	32.8
Holistic	14.5	21.7	25.5	29.5
Mean	22.4	28.2	32.3	36.6

Table 11. Success rates of MobileManiVLA on the G1 Robot with different state inputs.

Object	Unseen Object Unseen Scene	Unseen Object Seen Scene	Seen Object Unseen Scene	Seen Object Seen Scene
Laptop	72.5	90.0	73.8	87.5
Cabinet	22.3	30.0	56.8	65.7
Faucet	30.6	39.9	52.5	59.0
Table	19.3	25.3	57.5	61.2
Cart	23.5	33.1	44.5	50.5
Holistic	21.7	37.7	37.2	50.5
Mean	28.2	39.2	51.3	59.6

Table 12. Success rates of MobileManiVLA on the G1 Robot with seen or unseen objects and scenes.

whereas MobileManiVLA is evaluated on unseen objects and scenes, with 10 episodes per robot-object-skill-scene combination. Both experiments are conducted with randomized robot initial poses to assess robustness.

B.2. Ablation Studies.

We conduct ablation studies and model comparisons on a subset of MobileManiDataset that includes only the challenging skills: open, pull, and pick for the G1 robot, covering 272 training and 66 testing objects across 6 categories: laptop, cabinet, faucet, table, cart and holistic objects, providing 4,352 robot-object-skill-scene combinations for training and 264 unseen combinations for testing. All VLA models are trained with a batch size of 120 and 160K iterations, which are evaluated on unseen objects and scenes with 10 episodes per combination. The detailed success rates of MobileManiVLA on the G1 robot with different image inputs, state inputs, and unseen items are shown in Table 10, Table 11, and Table 12.



Figure 8. Real-world inference of MobileManiVLA on the G1 robot for the open laptop task.

Object	MobileManiVLA	$\pi_{0.5}$	π_0	CogACT	OpenVLA
Laptop	72.5	47.9	16.3	13.7	8.4
Cabinet	22.3	20.0	23.7	13.8	3.7
Faucet	30.6	23.3	16.5	6.0	4.3
Table	19.3	14.3	10.6	6.1	4.8
Cart	23.5	16.9	5.6	11.9	3.1
Holistic	21.7	9.7	4.5	4.2	3.5
Mean	28.2	18.8	11.2	6.8	4.5

Table 13. Model comparisons of representative VLA models with their default architectures and input modalities on the G1 robot.

B.3. Model Comparisons

For the VLA model comparisons in Table 6 of the main paper, we fine-tune all models using a unified action representation. Specifically, each model predicts a 6D end-effector pose along with a gripper open/close action. The batch size is fixed at 120, and each model is trained for 160K steps. The learning schedule for each model is set according to its recommended or default configuration.

Specifically, π_0 was optimized using a cosine decay schedule with a 1,000 step warmup, a peak learning rate of 2.5e-5, decay steps of 100K, and a final decay learning rate of 2.5e-6. The action chunk size was 50 steps, and execution was performed over 8 steps. $\pi_{0.5}$ used a cosine decay schedule with a 1,000 step warmup, a peak learning rate of 5e-5, decay steps of 100K, and a final decay learning rate of 5e-5, with an action chunk size of 16 steps and executes 8 steps. Both π_0 and $\pi_{0.5}$ took two RGB images (head-view and wrist-view) as input. *CogACT* employs a constant learning rate of 2e-5 with an action chunk size of 16 steps. *OpenVLA* predicted the next-step 7-dimensional action with a constant learning rate of 2e-5. Both *vallina CogACT* and *OpenVLA* use a single head-view RGB image as input and did not take the robot state as input.

C. Real-world VLA Inferences

C.1. Hardware Setup.

We inference our MobileManiVLA in the real-world on the G1 robot from AgiBot [?], which is equipped with dual-arms, a head-mounted camera capturing images at



Figure 9. Real-world setup of the G1 robot.

1280 \times 720, and two wrist-mounted cameras capturing images at 640 \times 480, as shown in Figure 9. To align with our simulation setting, we fix the left arm and only active the mobile base, right arm, and right gripper. All raw head-view and wrist-view RGB images are cropped to 480 \times 480 before being fed into the model.

Due to hardware limitations, AgiBot does not provide access to the wrist cameras' depth sensors, and the depth quality of the head camera is severely degraded. Therefore, for visual reliability, we adopt the MobileManipVLA variant that uses only the multi-view RGB images and hand pose state inputs, as reported in Table 10. This RGB only MobileManipVLA achieves a 40.8% success rate on the open laptop task but falls below 15% on all other tasks. To ensure safe deployment, our real-world inferences focus exclusively on the open laptop task.

C.2. VLA Inference Results.

For the open laptop task, we inference our MobileManiVLA with the robot base starts 1m away from the laptop. We inference the model over 10 trials with randomized robot pose initialization. During inference, MobileManiVLA receives the natural-language instruction "open laptop," real-time RGB images from the head and wrist cameras, and the real-time right-wrist pose expressed in the mobile base frame. Demonstrations of the RGB images used during inference are shown in Figure 8. The overall success rate achieved in the real world is 40% for the open laptop task.

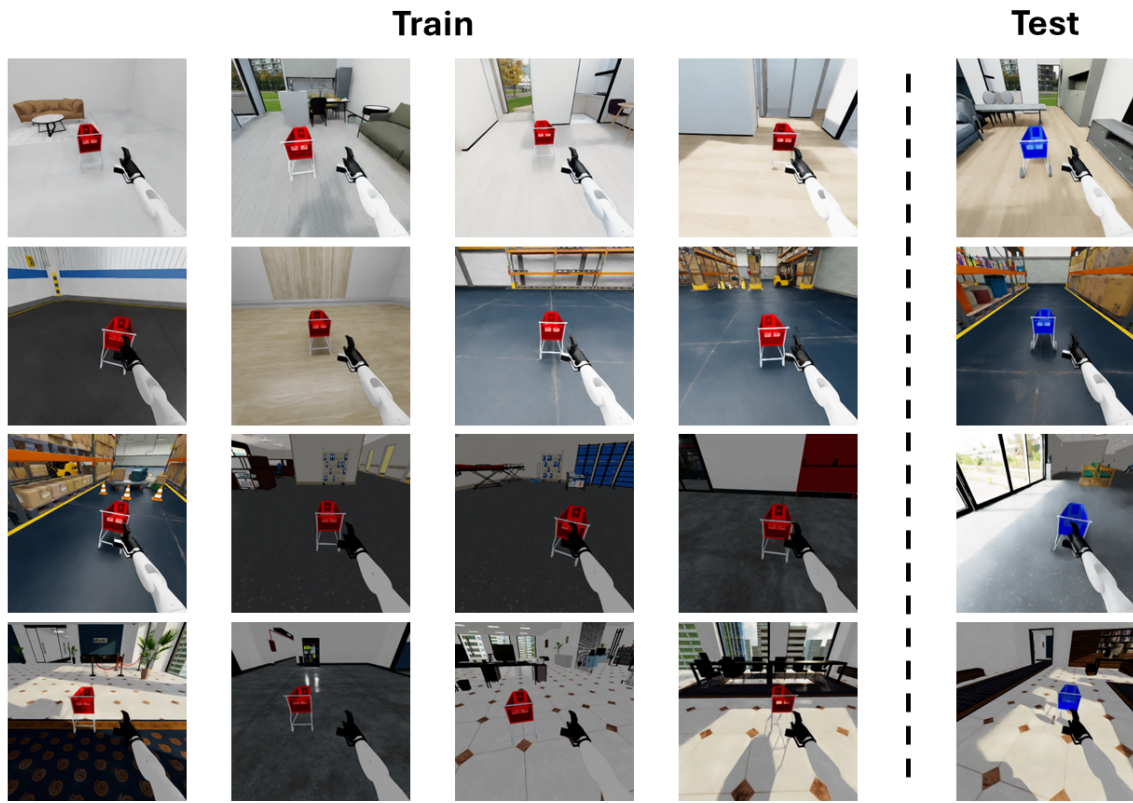


Figure 10. Realistic space scenes for cart.

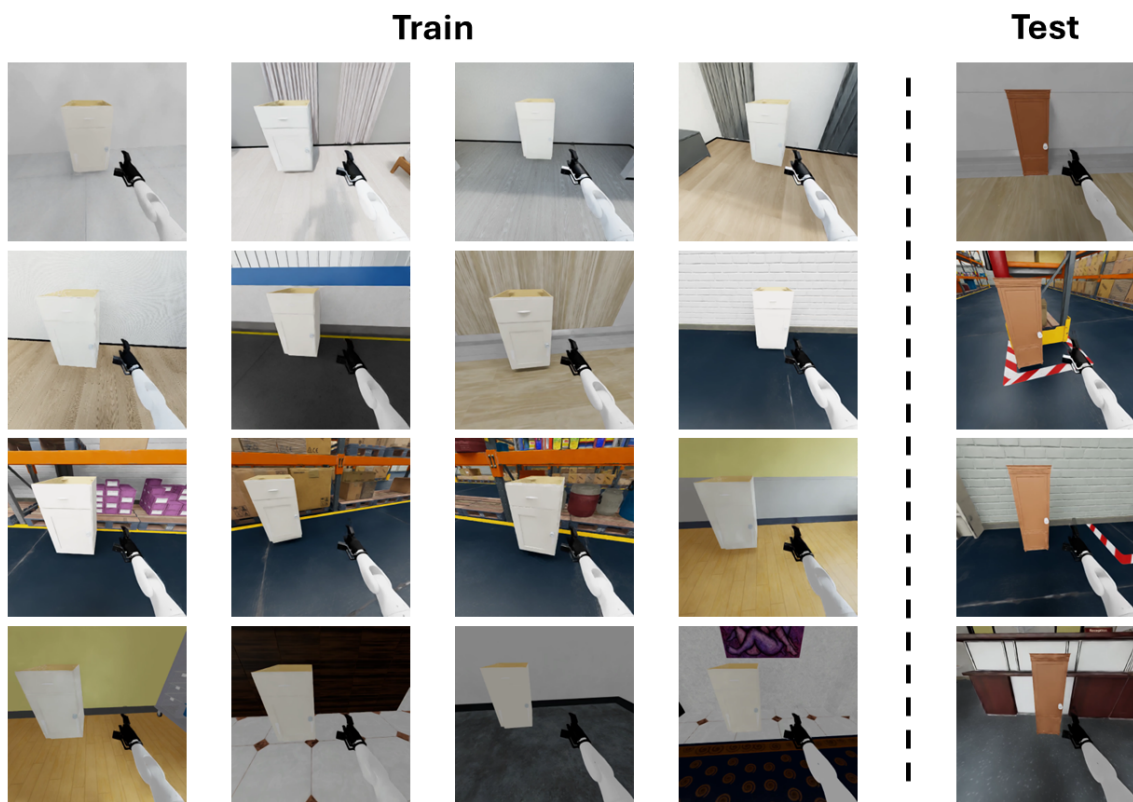


Figure 11. Realistic wall scenes for toilet, trashcan, refrigerator, washing machine, fridge, cabinet, table.

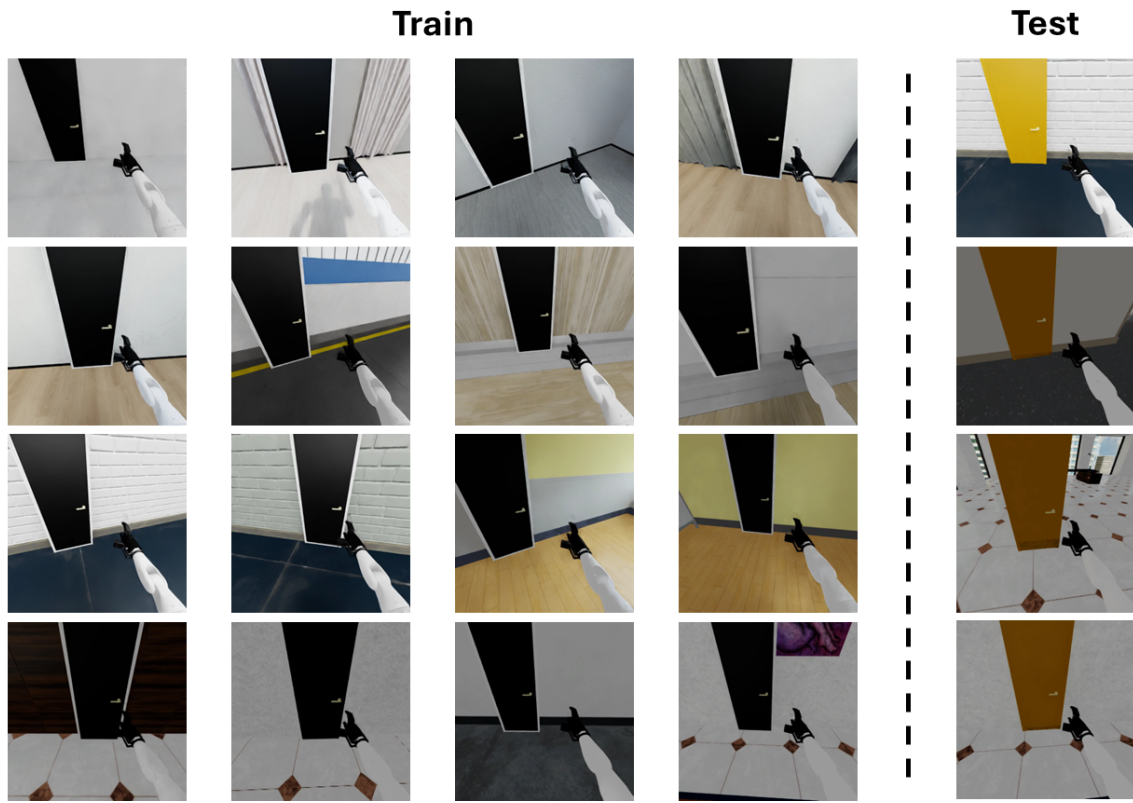


Figure 12. Realistic **door** scenes for window, lever door, round door.

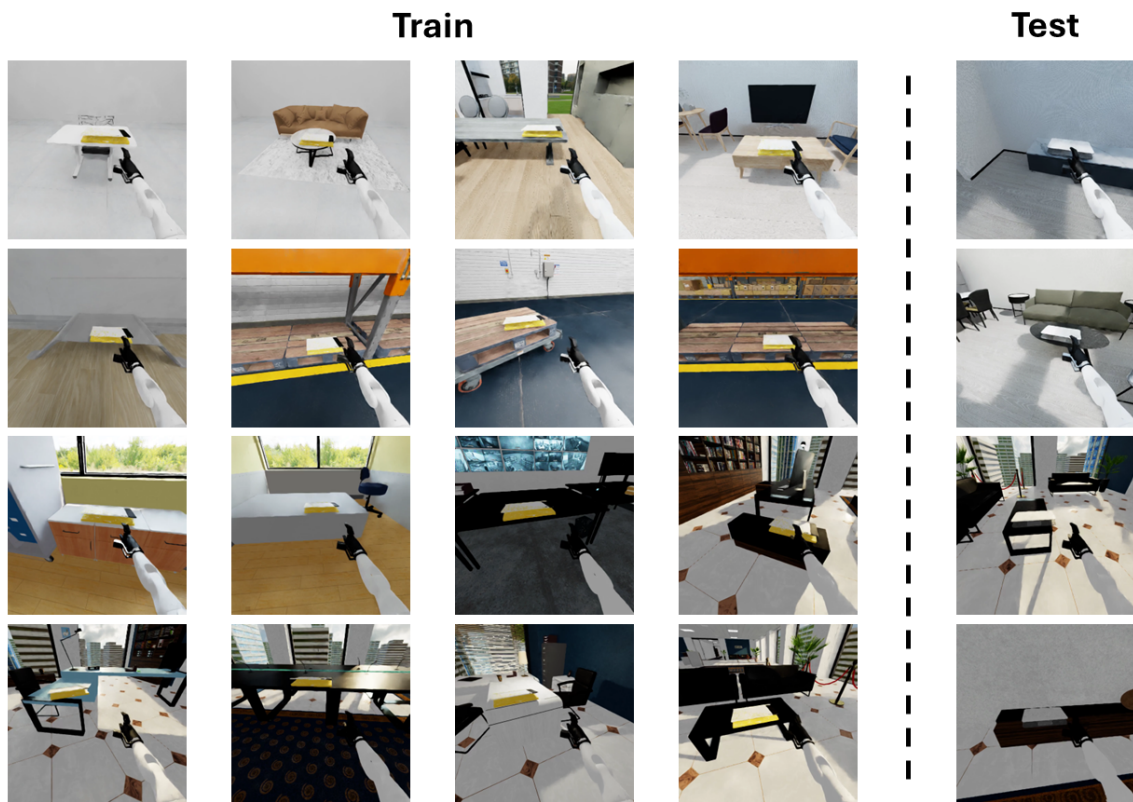


Figure 13. Realistic **tabletop** scenes for box, laptop, dishwasher, oven, microwave, safe, faucet, holistic objects.

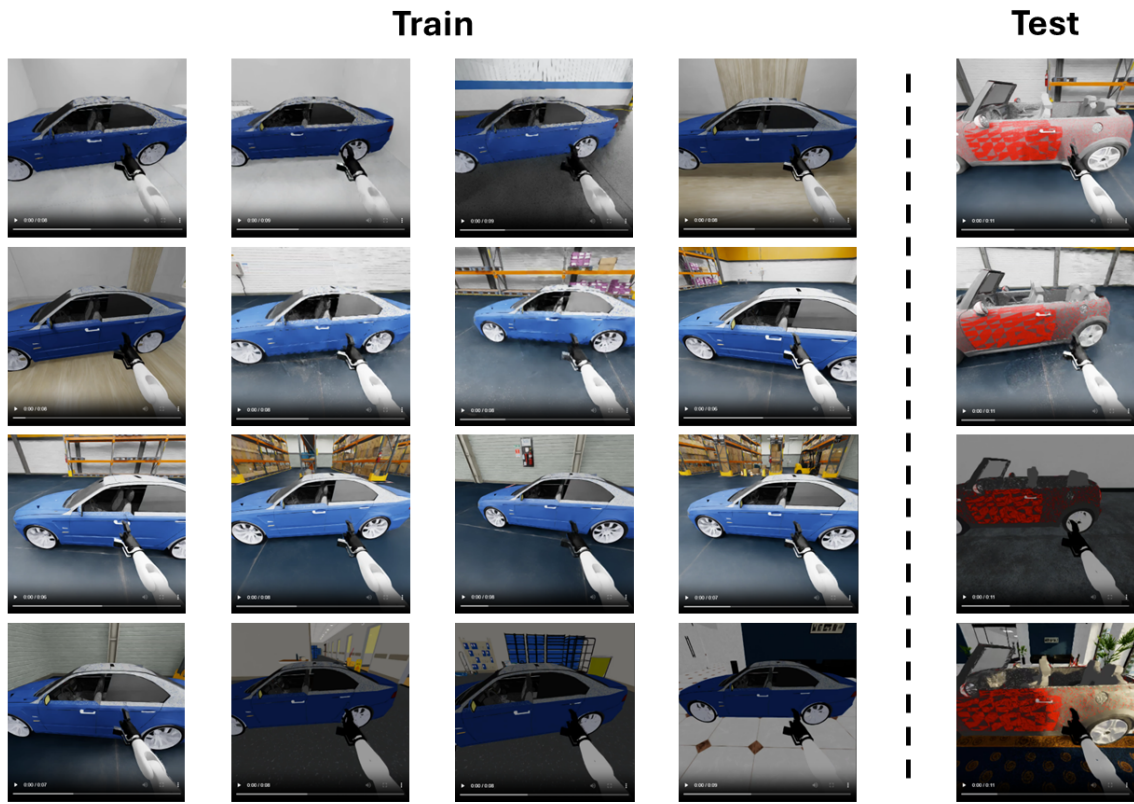
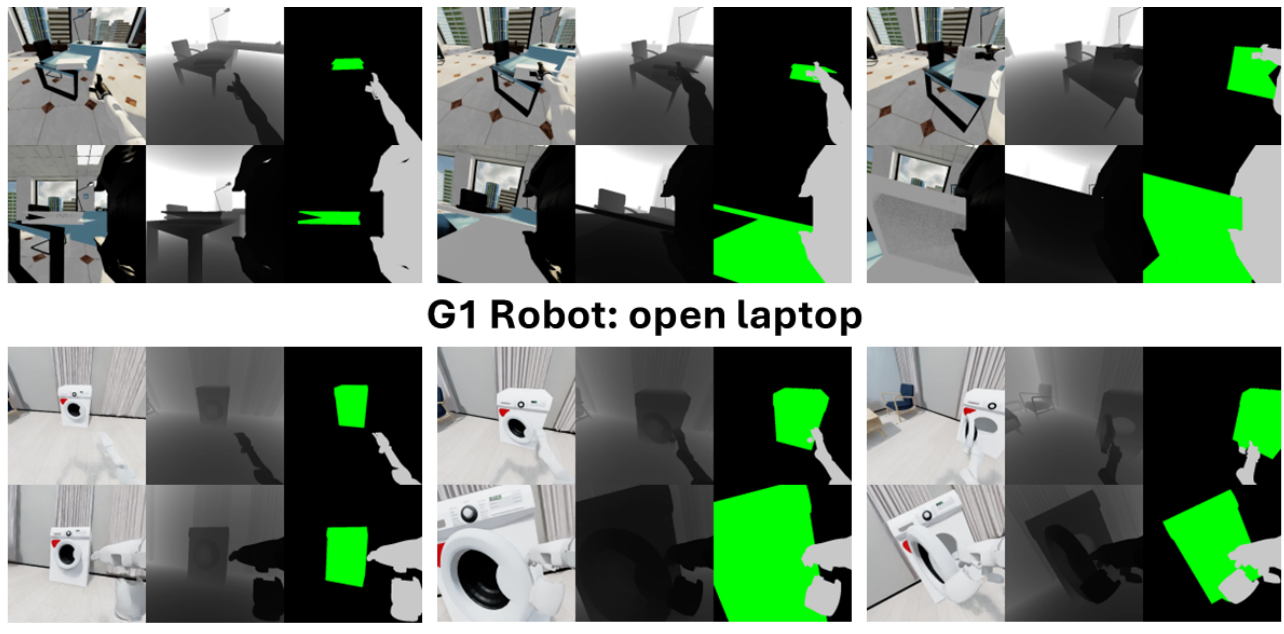


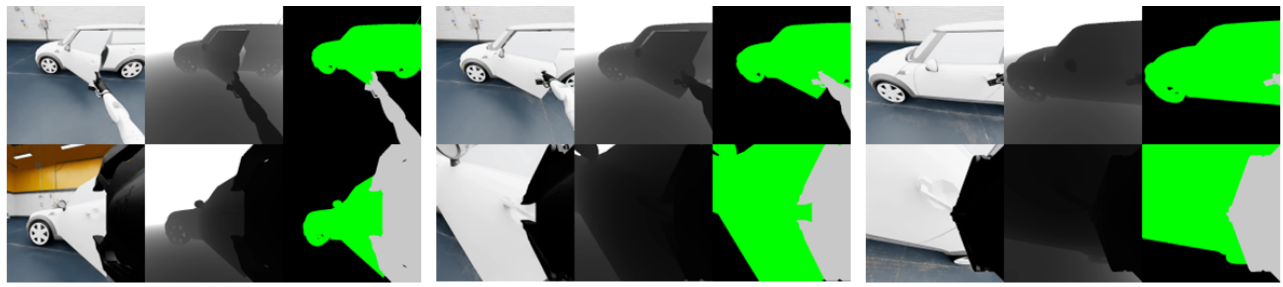
Figure 14. Realistic **outdoor** scenes for car.



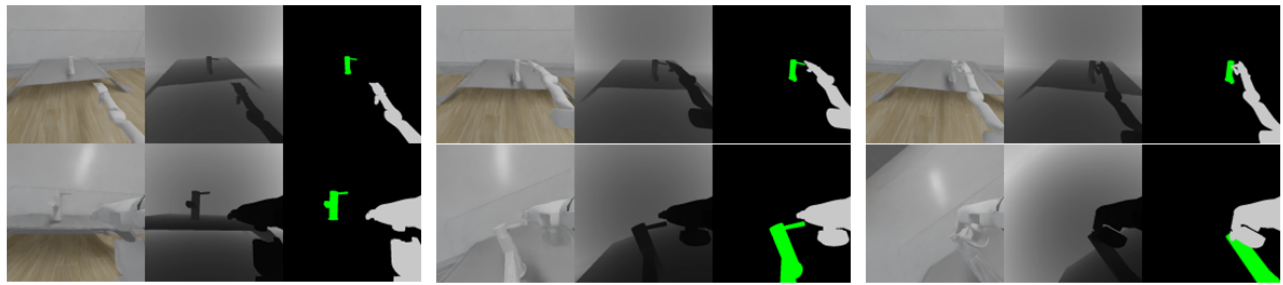
G1 Robot: open laptop

XHand Robot: open washing machine

Figure 15. **Open** trajectories from the G1 robot and the XHand robot.

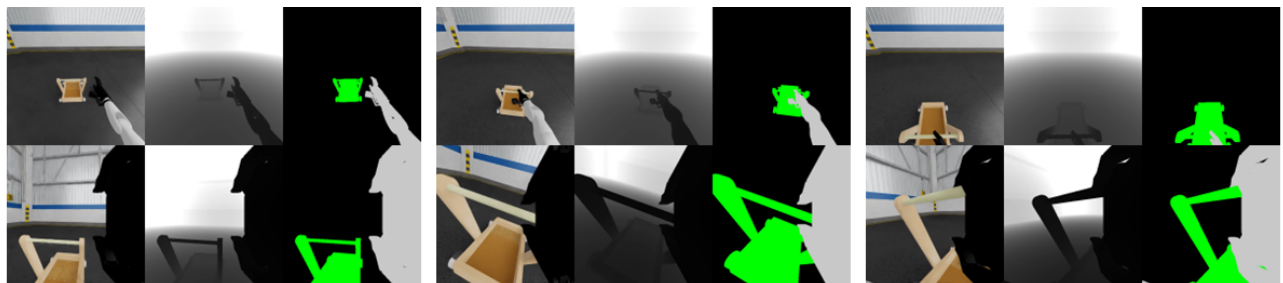


G1 Robot: close car

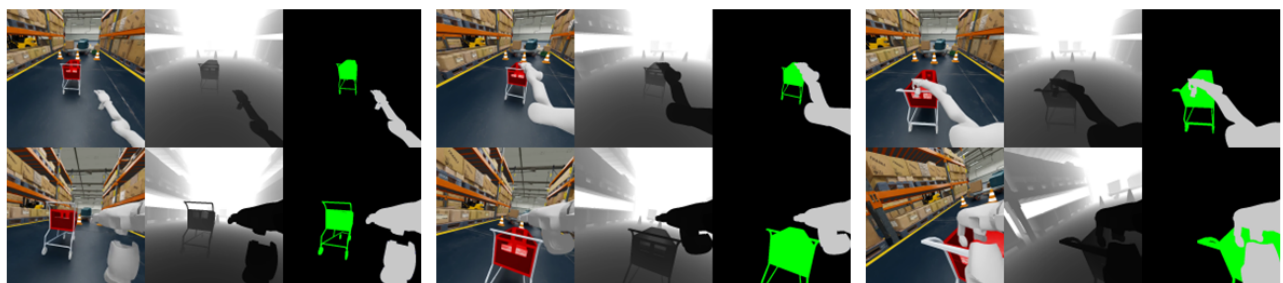


XHand Robot: close faucet

Figure 16. **Close** trajectories from the G1 robot and the XHand robot.

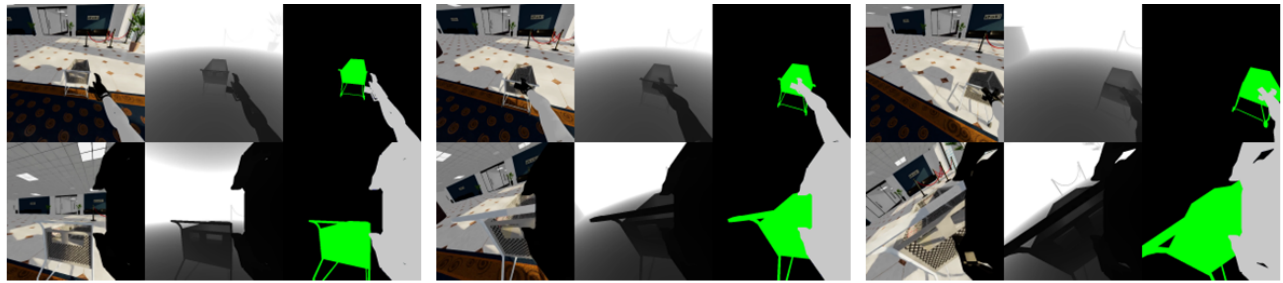


G1 Robot: pull cart

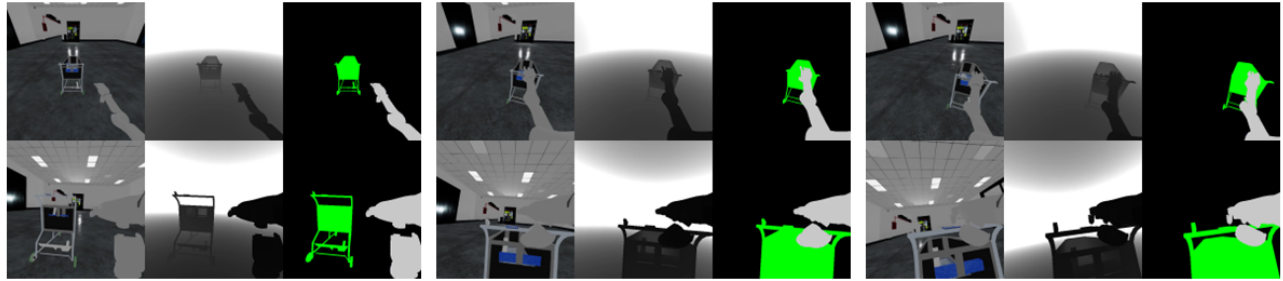


XHand Robot: pull cart

Figure 17. **Pull** trajectories from the G1 robot and the XHand robot.

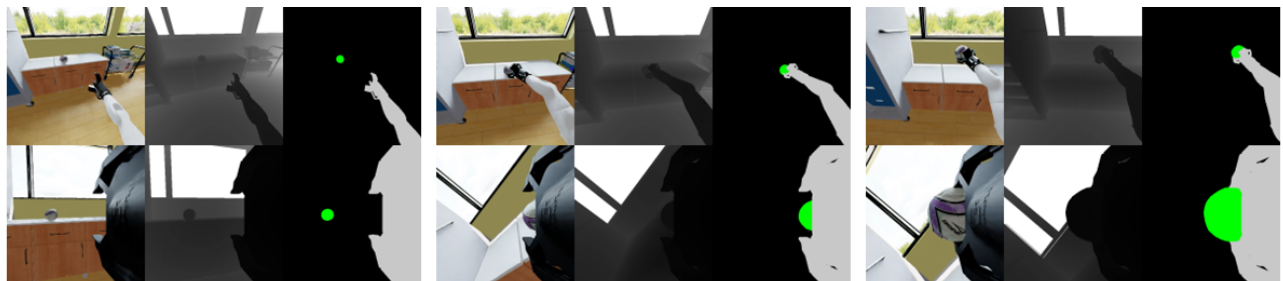


G1 Robot: push cart

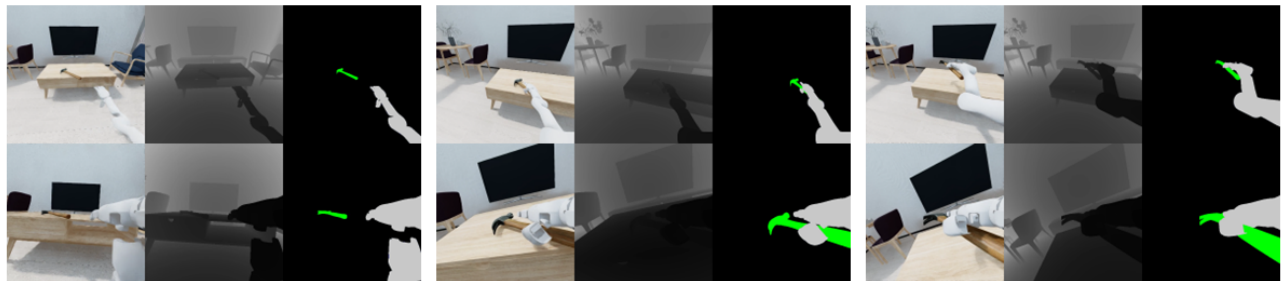


XHand Robot: push cart

Figure 18. **Push** trajectories from the G1 robot and the XHand robot.



G1 Robot: pick mini soccer ball



XHand Robot: pick hammer

Figure 19. **Pick** trajectories from the G1 robot and the XHand robot.